REPORT DOCUMENTATION PAGE

Form Approved OMB NO. 0704-0188

1. REPORT DATE (DD-MM-YYYY)	2. REPORT TYPE	3. DATES COVERED (From - To)
31-10-2011	Final Report	27-Jun-2008 - 30-Oct-2011

4. TITLE AND SUBTITLE
Milli-Biology

5a. CONTRACT NUMBER
W911NF-08-1-0254

5b. GRANT NUMBER

5c. PROGRAM ELEMENT NUMBER
8D10AN

6. AUTHORS
Neil Gershenfeld

5d. PROJECT NUMBER

5e. TASK NUMBER

5f. WORK UNIT NUMBER

7. PERFORMING ORGANIZATION NAMES AND ADDRESSES
Massachusetts Institute of Technology (MIT)
Office of Sponsored Programs
Bldg. E19-750
Cambridge, MA 02139 -4307

8. PERFORMING ORGANIZATION REPORT NUMBER

9. SPONSORING/MONITORING AGENCY NAME(S) AND ADDRESS(ES)
U.S. Army Research Office
P.O. Box 12211
Research Triangle Park, NC 27709-2211

10. SPONSOR/MONITOR'S ACRONYM(S)
ARO

11. SPONSOR/MONITOR'S REPORT NUMBER(S)
54534-MS-DRP.1

12. DISTRIBUTION AVAILIBILITY STATEMENT
Approved for Public Release; Distribution Unlimited

13. SUPPLEMENTARY NOTES
The views, opinions and/or findings contained in this report are those of the author(s) and should not contrued as an official Department of the Army position, policy or decision, unless so designated by other documentation.

14. ABSTRACT
The milli-biology project was inspired by the existence proof for programmable matter, molecular biology. Macroscopic organisms are full of microscopic machinery, assembled from nanostructures. The heart of how this happens is protein folding in the ribosome, where a one-dimensional mRNA codes for the assembly of a three-dimensional functional protein by linking amino acids. Milli-biology sought to re-implement this natural workflow with engineered materials, in order to expand the range of length scales and properties beyond what is

15. SUBJECT TERMS
programmable matter

16. SECURITY CLASSIFICATION OF:			17. LIMITATION OF ABSTRACT	15. NUMBER OF PAGES	19a. NAME OF RESPONSIBLE PERSON
a. REPORT	b. ABSTRACT	c. THIS PAGE			Neil Gershenfeld
UU	UU	UU	UU		19b. TELEPHONE NUMBER 617-253-7680

Report Title

Milli-Biology

ABSTRACT

The milli-biology project was inspired by the existence proof for programmable matter, molecular biology. Macroscopic organisms are full of microscopic machinery, assembled from nanostructures. The heart of how this happens is protein folding in the ribosome, where a one-dimensional mRNA codes for the assembly of a three-dimensional functional protein by linking amino acids. Milli-biology sought to re-implement this natural workflow with engineered materials, in order to expand the range of length scales and properties beyond what is available in organic chemistry.

Enter List of papers submitted or published that acknowledge ARO support from the start of the project to the date of this printing. List the papers, including journal references, in the following categories:

(a) Papers published in peer-reviewed journals (N/A for none)

Received Paper

TOTAL:

Number of Papers published in peer-reviewed journals:

(b) Papers published in non-peer-reviewed journals (N/A for none)

Received Paper

TOTAL:

Number of Papers published in non peer-reviewed journals:

(c) Presentations

Number of Presentations: 0.00

Non Peer-Reviewed Conference Proceeding publications (other than abstracts):

Received Paper

TOTAL:

Number of Non Peer-Reviewed Conference Proceeding publications (other than abstracts):

Peer-Reviewed Conference Proceeding publications (other than abstracts):

Received Paper

TOTAL:

Number of Peer-Reviewed Conference Proceeding publications (other than abstracts):

(d) Manuscripts

Received	Paper

TOTAL:

Number of Manuscripts:

Books

Received	Paper

TOTAL:

Patents Submitted

Actuators and Motors using Electropermanent Magnets
Cellular Automotion

Patents Awarded

Awards

Graduate Students

NAME	PERCENT_SUPPORTED	Discipline
Ara Knaian	1.00	
Kenny Cheung	1.00	
Maxim Lobovsky	1.00	
Amy Sun	1.00	
FTE Equivalent:	**4.00**	
Total Number:	**4**	

Names of Post Doctorates

NAME	PERCENT_SUPPORTED
FTE Equivalent:	
Total Number:	

Names of Faculty Supported

NAME	PERCENT_SUPPORTED	National Academy Member
Joe Jacobson	0.10	
Neil Gershenfeld	0.10	
Erik Demaine	0.10	
George Church	0.10	
FTE Equivalent:	**0.40**	
Total Number:	**4**	

Names of Under Graduate students supported

NAME	PERCENT SUPPORTED	Discipline
Asa Oines	1.00	EECS
Peter Schmidt-Nielsen	1.00	EECS
FTE Equivalent:	**2.00**	
Total Number:	**2**	

Student Metrics

This section only applies to graduating undergraduates supported by this agreement in this reporting period

The number of undergraduates funded by this agreement who graduated during this period:	0.00
The number of undergraduates funded by this agreement who graduated during this period with a degree in science, mathematics, engineering, or technology fields:.....	0.00
The number of undergraduates funded by your agreement who graduated during this period and will continue to pursue a graduate or Ph.D. degree in science, mathematics, engineering, or technology fields:.....	0.00
Number of graduating undergraduates who achieved a 3.5 GPA to 4.0 (4.0 max scale):	0.00
Number of graduating undergraduates funded by a DoD funded Center of Excellence grant for Education, Research and Engineering:	0.00
The number of undergraduates funded by your agreement who graduated during this period and intend to work for the Department of Defense	0.00
The number of undergraduates funded by your agreement who graduated during this period and will receive scholarships or fellowships for further studies in science, mathematics, engineering or technology fields:	0.00

Names of Personnel receiving masters degrees

NAME	
Ara Knaian	
Maxim Lobovsky	
Total Number:	**2**

Names of personnel receiving PHDs

NAME	
Ara Knaian	
Total Number:	**1**

Names of other research staff

NAME	PERCENT SUPPORTED
John DiFrancesco	0.25
Joe Murphy	0.10
Jonathan Bachrach	0.50
Saul Griffith	0.25
FTE Equivalent:	**1.10**
Total Number:	**4**

Sub Contractors (DD882)

Inventions (DD882)

Scientific Progress

see attachment

Technology Transfer

Milli-Biology

Programmable Matter
W911NF-08-1-0254
Final Report
October 30, 2011

Introduction

The milli-biology project was inspired by the existence proof for programmable matter, molecular biology. Macroscopic organisms are full of microscopic machinery, assembled from nanostructures. The heart of how this happens is protein folding in the ribosome, where a one-dimensional mRNA codes for the assembly of a three-dimensional functional protein by linking amino acids. Milli-biology sought to re-implement this natural workflow with engineered materials, in order to expand the range of length scales and properties beyond what is available in organic chemistry.

A central result from the project was a proof of the universality of folding a one-dimensional string into an arbitrary connected three-dimensional structure. This was embodied in a constructive workflow from a CAD design file to a linear folding code. Coded folding was then investigated in systems with sizes spanning 9 orders of magnitude, from small proteins to large robots.

A program focus was the development of a family of "motein" mechanical proteins. These are built as a continuous one-dimensional structure of linked cells that can locally compute, communicate, and fold. They were made with feature sizes ranging from millimeters to meters, all able to execute the same folding codes.

The effort to scale moteins to smaller sizes led to the invention of electropermanent actuators, in which a hard magnet biases a softer magnet, so that its hysteresis loop passes through the origin. A conventional electromechanical motor is maximally inefficient at low RPM because power is wasted as heat in the coils, requiring gearing at low RPM, and power is required to maintain static position, requiring holding brakes. But this is exactly the regime needed for programmable materials; electropermanent motors are efficient at low RPM because each step is a discrete domain flip, and hold position without power because of the static magnetization.

To program programmable matter, the project investigated reconfigurability in spatial programming languages. This resulted in the development of Reconfigurable Asynchronous Logic Automata. RALA adds to non-reconfigurable Asynchronous Logic Automata a "stem" cell that can convert state tokens into cell configurations. This explicit linkage between computation and geometry was used to implement a workflow from three-dimensional designs to a one-dimensional ALA program code to construct them, and self-reproducing programs such as replicator loops.

As the project progressed, a distinction was drawn between between two senses of programmable matter: online real-time shape changes, versus offline but rapid (re)configuration. The latter was based on assembling digital materials, which can be thought of as externally-programmable matter. This can be realized with much simpler elements; prototypes of these and their assembly processes were developed. Workflows developed by the project for coded folding and assembly also found broad application in passive construction processes.

These results are described in subsequent sections on Folding, Moteins, RALA, Digital Materials, Microfluidics, Molecular Assembly, Infrastructure, Conclusions, and Publications.

Folding

Any shape can be programmatically formed from a discrete set of polygonal or polyhedral components. This provides a strategy for making programmable matter in the form of shape-universal strings, as strings of identical blocks that simply fold onto each other according to the desired global shape. Given lattice geometries and a strategy for generating space-filling curves, reconfigurable robotic systems can be adapted to chained formats, with the advantage of reduced required degrees of freedom per unit, a low number of states per unit, and a power, structural, and communications backbone. It is noted that non-Euclidean space tilings are just as suited to these algorithms.

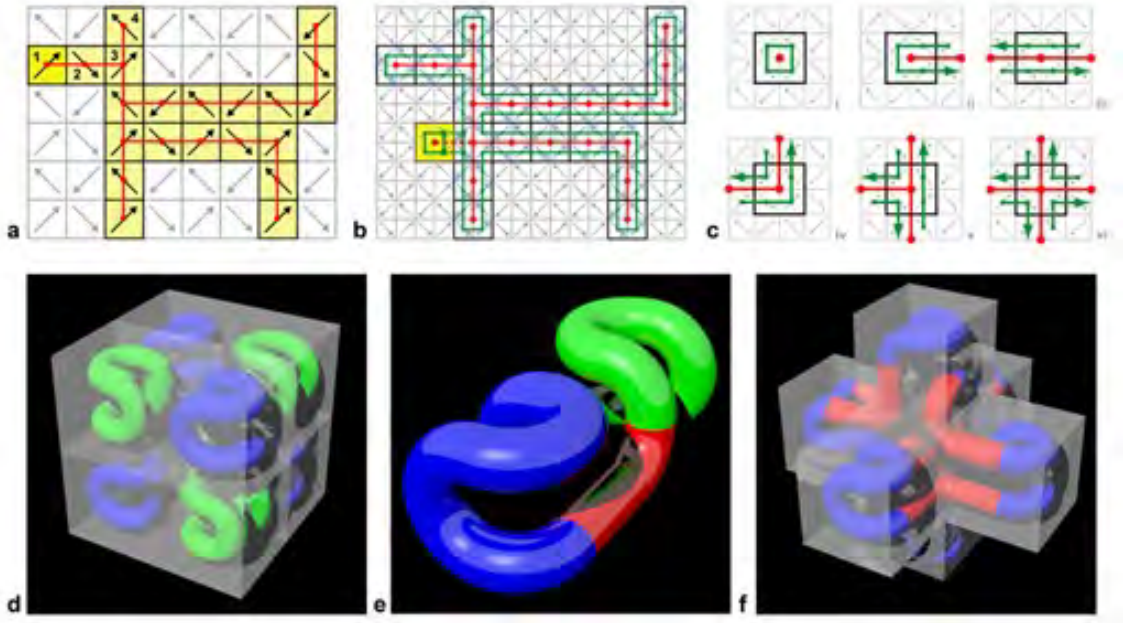

Hamiltonian Circuit construction rules for simple cubic lattice.

For universal shape making, we may start with any common three-dimensional CAD file evaluated over a lattice. Then, the spanning graph and space-filling curve is

constructed using this lattice, which is processed into the code for the string. The intractable Hamiltonian path problem becomes tractable with a spatial subdivision. A key aspect of the system is that each unit solves for a local solution – the global solution is a product of the aggregated local results of the programs of each unit. The resulting program is as simple as: "turn left or right until you touch your previous neighbor," for each unit. We call these shape-universal reconfigurable strings "moteins", for motorized proteins.

Automated path construction from an arbitrary shape.

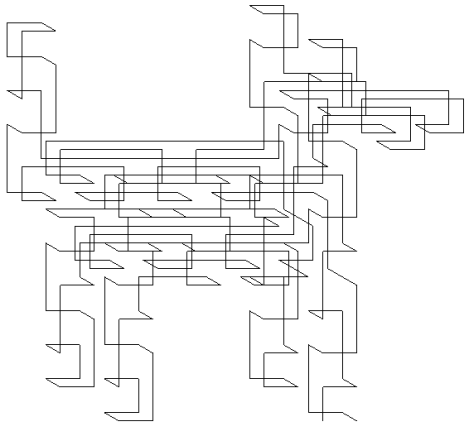

Automated generation of Hamiltonian Circuit for a three dimensional shape.

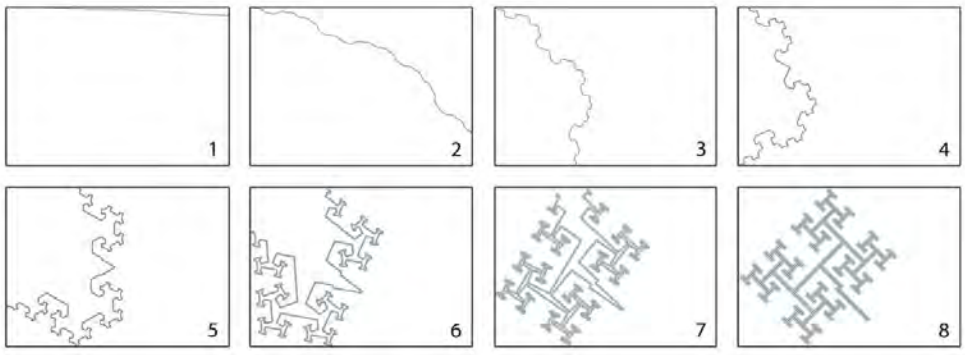

Frames showing progress of a two dimensional motein string folding into a fractal antenna shape.

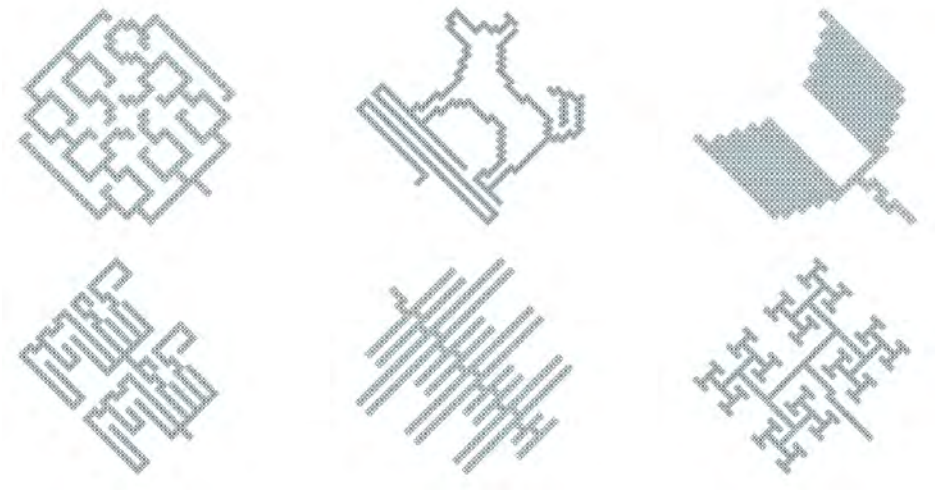

Examples of antenna shapes accessible from the same string.

Hexagonally-Bisected Cube

The design of some of the moteins - which were fabricated as testbeds - packs on a simple cubic lattice (C-motein) in any of its (upper bound $3O(n)$, for n length string) configurations. Each rigid unit along the string is comprised of two halves of adjacent cubes in this final lattice. These halves are formed from the regular hexagonal bisection of the cube. Each unit rotates about the central axis that is orthogonal to this bisection plane, and with respect to the previous adjacent unit along the string.

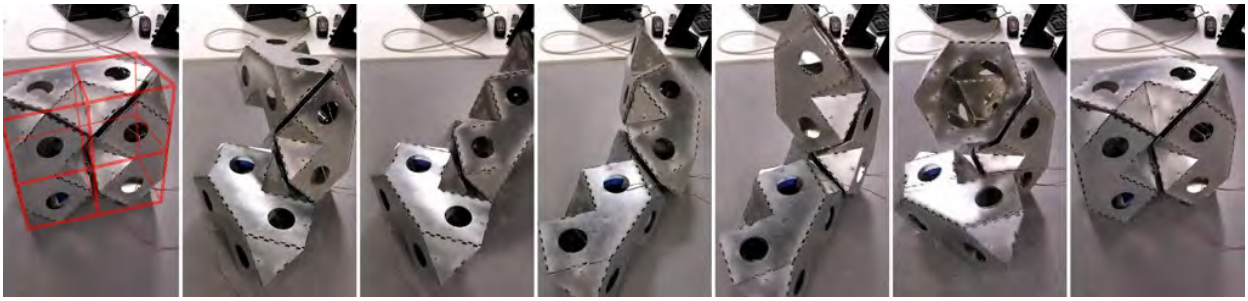

Early cubic motein (C-motein) powered prototype packing on a cubic lattice.

This hexagonally bisected cube kinematic geometry was first shown in reconfigurable robotics with the molecube system, with reconfigurable connections on cubic modules. In a chain configuration, this is also similar to the Rubik's Snake toy, but with modules that closely pack on a cubic lattice and accordingly with a larger dihedral angle between bearing faces.

Moteins form shape-universal programmable chains; this design uses a single degree of freedom, and only two goal states per unit. The chain configuration allows for a wired power and communication backbone, and allows spatial interconnect to be utilized for other functions (i.e. purely structural interconnect, carrying payloads, etc.). Multiple

units along the same string can be programmed to cooperate and perform force and spatial transformation multiplexing.

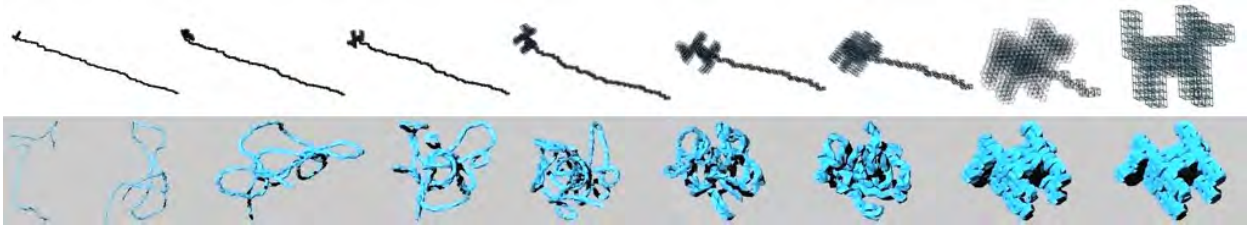

Simulated folding strategies for C-moteins.

8 unit motein with 27 cubic inch unit size.

Right-Angle Tetrahedron

The Right-Angle Tetrahedron is another space filling polyhedron. When hinged in series by the edges along their two right spatial angles, they can also form foldable space-tiling chains.

Right-angle tetraheda.

6-monomer long segments of such chains can be folded into rhombical hexahedra.

Folding of right-angle tetrahedra into space-filling rhombical hexahedra.

We showed that right-angle tetrahedra have a number of useful construction properties:

- In a folded configuration, there is always an even number of modules between any two coincident hinges.
- Because any chain segment connecting any two coincident hinges always has an even number of modules, the only case of resulting face alignment is when the face of an even module aligns with a face of an odd module.
- Every three consecutive hinges are mutually orthogonal.
- Every two hinges separated by a multiple of 3 hinges are parallel to each other.
- Every two aligned hinges are separated by a multiple of 6 hinges.

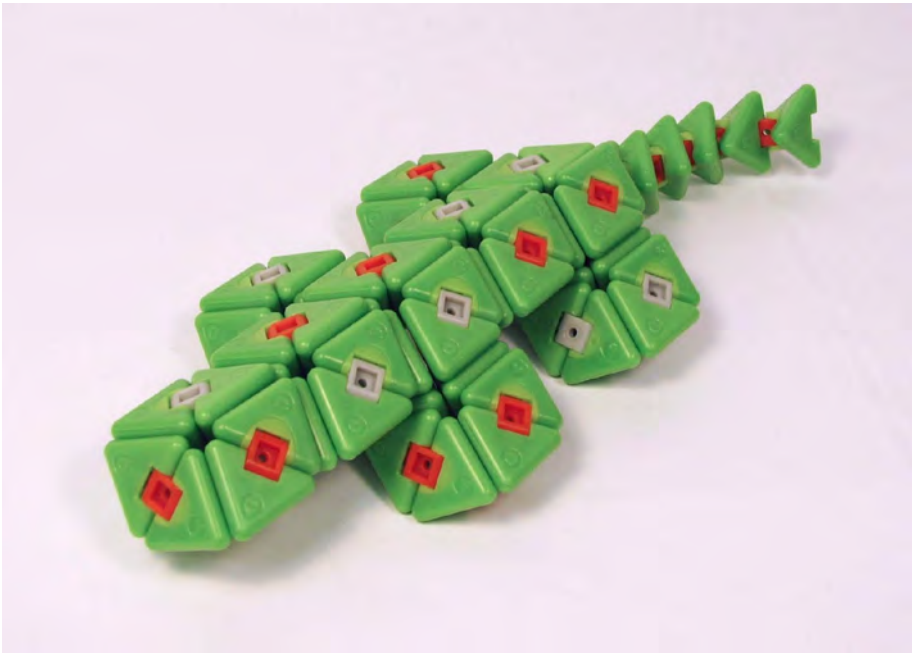

Folded right-angle tetrahedron chain.

Folding Workflow

Folding chains of hinged polyhedra into arbitrary 3D solids requires that we complete two tasks: (1) take a description of a target solid, for example in the form of a closed triangular surface mesh, and produce a final configuration including target positions for monomers and joint angles for the joints so that the chain forms a Hamiltonian path through the shape; and (2) plan for folding the monomers from an unfolded configuration into the final configuration. Specific procedures include rasterization of a target 3D shape, generation of a Hamiltonian path that visits all internal voxels of the target shape, along which the chain robot segments will be lined up in the folded configuration, and, finally, design of a folding trajectory for the chain robot.

Configuration

Space can be broken up into pixels for 2D and voxels for 3D, where pixels/voxels are the cells in a 2D/3D grid respectively. Rasterization is the process of placing a grid over a given shape and determining which voxels are inside and which voxels are outside of the shape. For little more effort we can determine for each voxel the minimum distance to the surface with interior voxels assigned negative values, exterior voxels assigned positive values, and boundary voxels assigned zero values. This array of distances is called a level set.

Our technique for calculating the level set values involves ray tracing. Shapes are input in STL format specifying a triangulated surface on the boundary of a given solid object. Any such triangulated surface file format will do. For every cell in the grid six rays are shot in each of the axis aligned directions while calculating the intersections with the triangulated surface. The minimum distance of these six values is recorded along with its sign according to the parity of the total number of intersections in any one direction. An odd number of intersections means the point is inside the shape and an even number means the point is outside.

Rasterizing cubic voxels is straightforward while rasterizing for right-angled tetrahedral monomers is more challenging. We can simplify the problem by making the tetrahedral voxel be a rhombic hexahedron comprised of six tetrahedra. By using a simple affine transformation we can transform a cubic grid into a hexahedral grid.

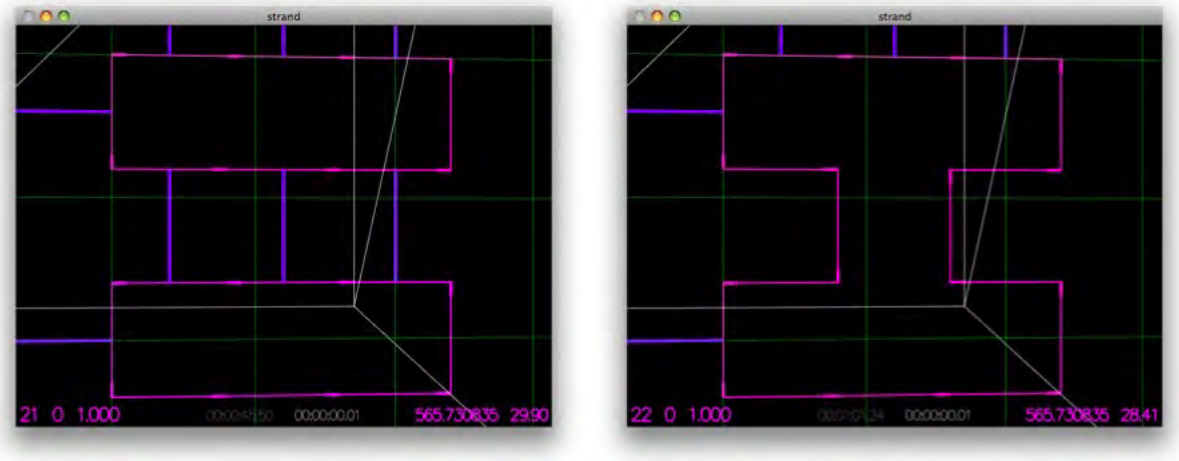

Merging of two paths along a parallel neighboring line segment.

Our approach to constructing a Hamiltonian path is to incrementally merge increasingly bigger paths. The algorithm starts with minimal local paths and incrementally merges neighboring paths. In two dimensions, the algorithm starts with 2x2 squares within the given 2D shape and then proceeds to merge neighboring squares forming bigger and bigger paths. Eventually the path visits every pixel in the shape.

Paths can be merged if they share a parallel neighboring line segment. In this case, surgery can be performed on the two paths A and B at the parallel line segments to route the flow between the two paths. In particular, the path would be diverted at the parallel line segments instead going from A to B at the beginning of the segment and then back from B to A at the end of the segment.

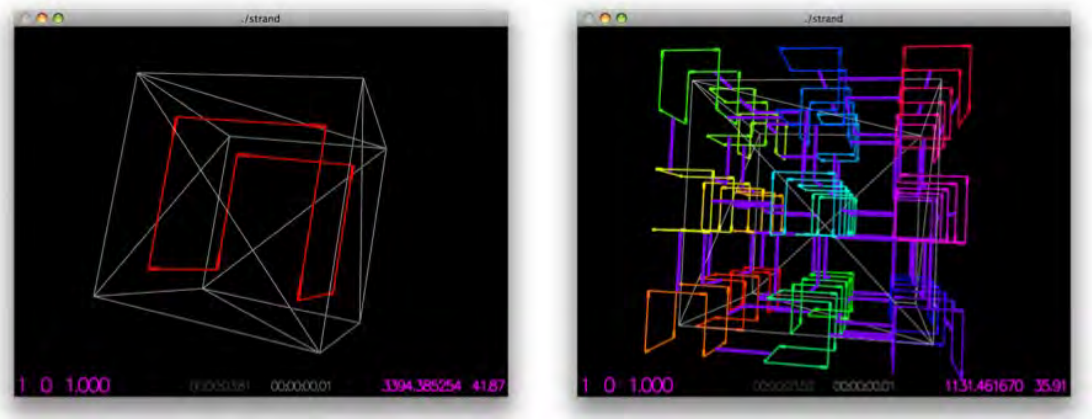

Initial mini path and initial orientation of mini paths.

In order to guarantee that we can find 2x2 mini paths, we must first rasterize at half the resolution and then divide the resulting pixels into four subpixels, that is 2x in each dimension. We call these metamodules and having metamodules ensures that there are a complete set of compatible initial mini paths.

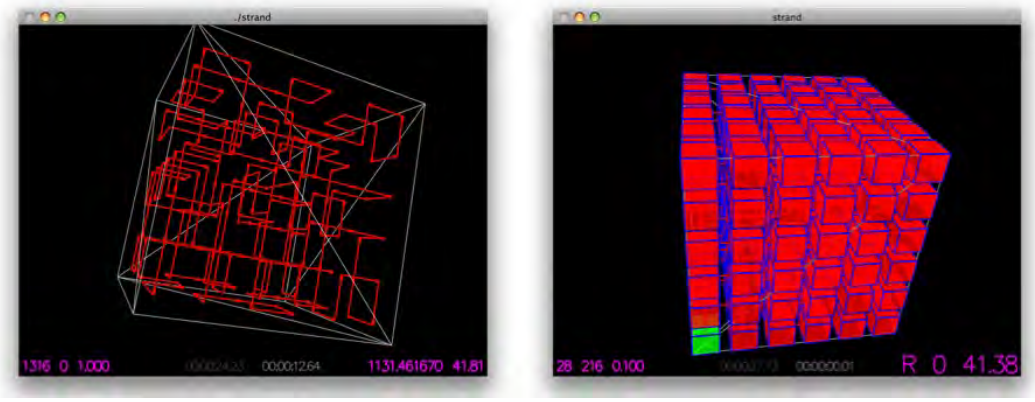

Final Hamiltonian path and resulting 216 cube chain on a 6x6 grid.

This algorithm also works in 3D by starting with mini paths over eight neighboring cells. If the orientation of the initial mini paths alternate with the parity of (x + y + z) (i.e., 3D checker board) then the algorithm never gets stuck. All mini paths have at least one compatible edge with their neighbors, unlike the naive implementation with all mini paths having identical orientation. The merging of two paths can never affect the exterior compatibility of remaining paths (including the newly merged path).

Hamiltonian path construction works on the tetrahedral chain by first constructing mini paths along the center of the six tetrahedral modules in each rhombic hexahedron used in the initial rasterization process. Each rhombic hexahedron can be viewed as a squashed cube and as such has six rhombic hexahedron neighbors, where each face is comprised of two tetrahedral faces and one hinge joint. Merging occurs between hexahedral faces and involves an analogous surgery to redirect the tour between the neighboring rhombic hexahedral metamodules.

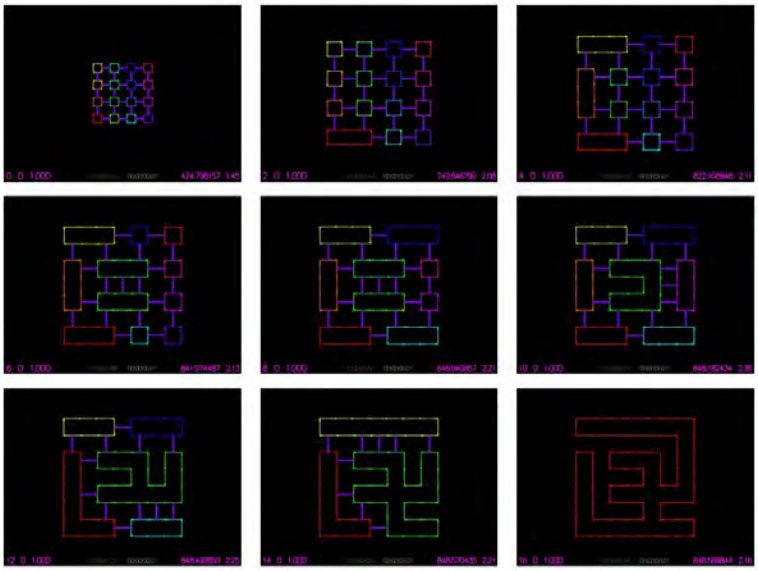

Incremental bottom-up path merging on a 8x8 grid filling a square. Each path has a unique color and purple lines depict the neighborhood relationship.

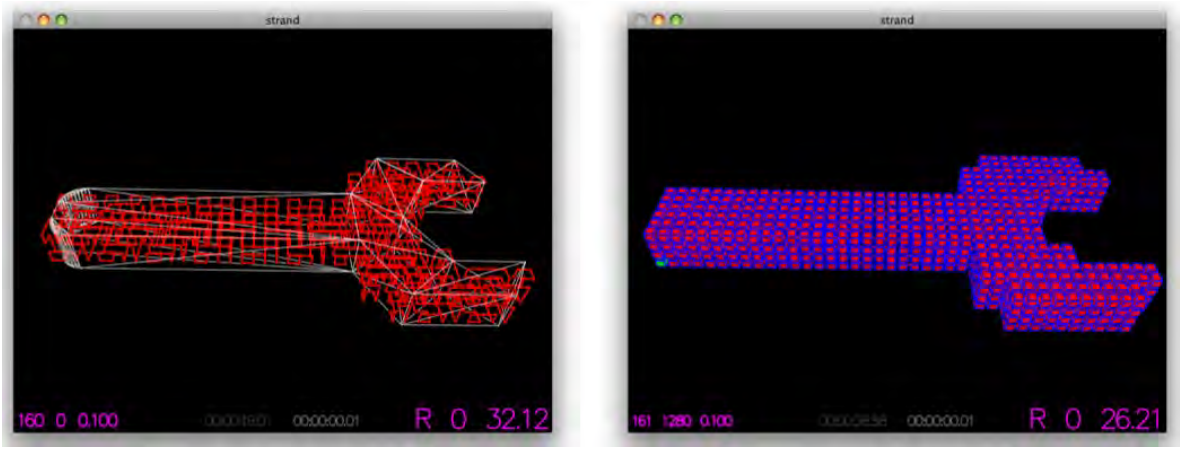

Hamiltonian path and resulting 1280 cube chain using cubic geometry on a wrench solid.

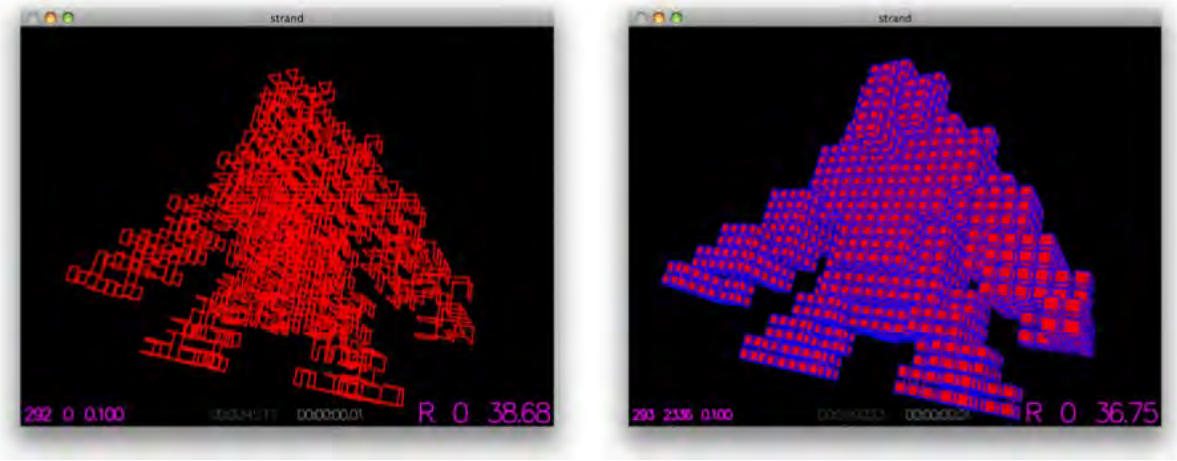

Hamiltonian path and resulting 2336 cube chain using cubic geometry on a gorilla solid.

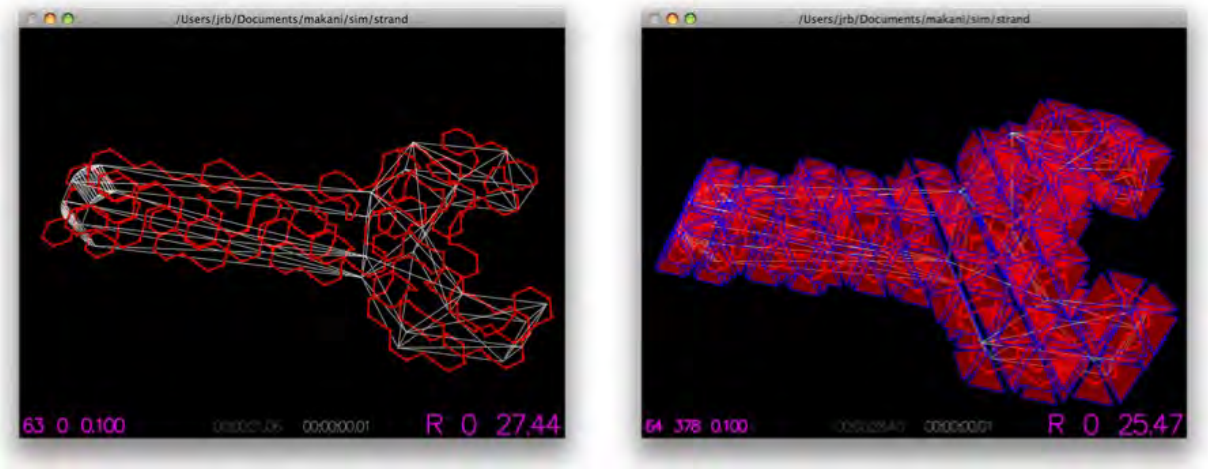

H

Hamiltonian path and resulting 62 tetrahedral chain using tetrahedral geometry on a wrench solid.

Path Planning

It is be easier to unfold than to fold. For path planning, we start from the target configuration, explode the chain while recording the joint angles, and servo to the angle snapshots in reverse.

To implement this approach, in simulation we start with the chain folded into its final configuration. We then apply radial forces to modules emanating from the center-of-mass of the entire ensemble. The motors on the joints are turned off and the joints themselves merely enforce their module-to-module constraints. While moving outwards at regular intervals we record a snapshot of joint angles across the chain. We stop when the chain has reached a fully unfolded straight configuration. We now have a complete record of the unfolding as a sequence of angle snapshots.

This unfolding sequence can be used to fold the chain by playing it back in reverse. This can be done again in simulation or for playback on a real robot. Each snapshot acts as a target to which we servo until the largest angle error is less than a given threshold. We need to servo with low enough stepsize and sufficient damping to have the actual folding trajectory mirror the unfolding trajectory so as to not cause tangling. In order to lower the chance of tangling we introduce a repelling force between unconnected modules during the unfolding. Thus the modules not only explode from the center but also maintain distance from nearby modules.

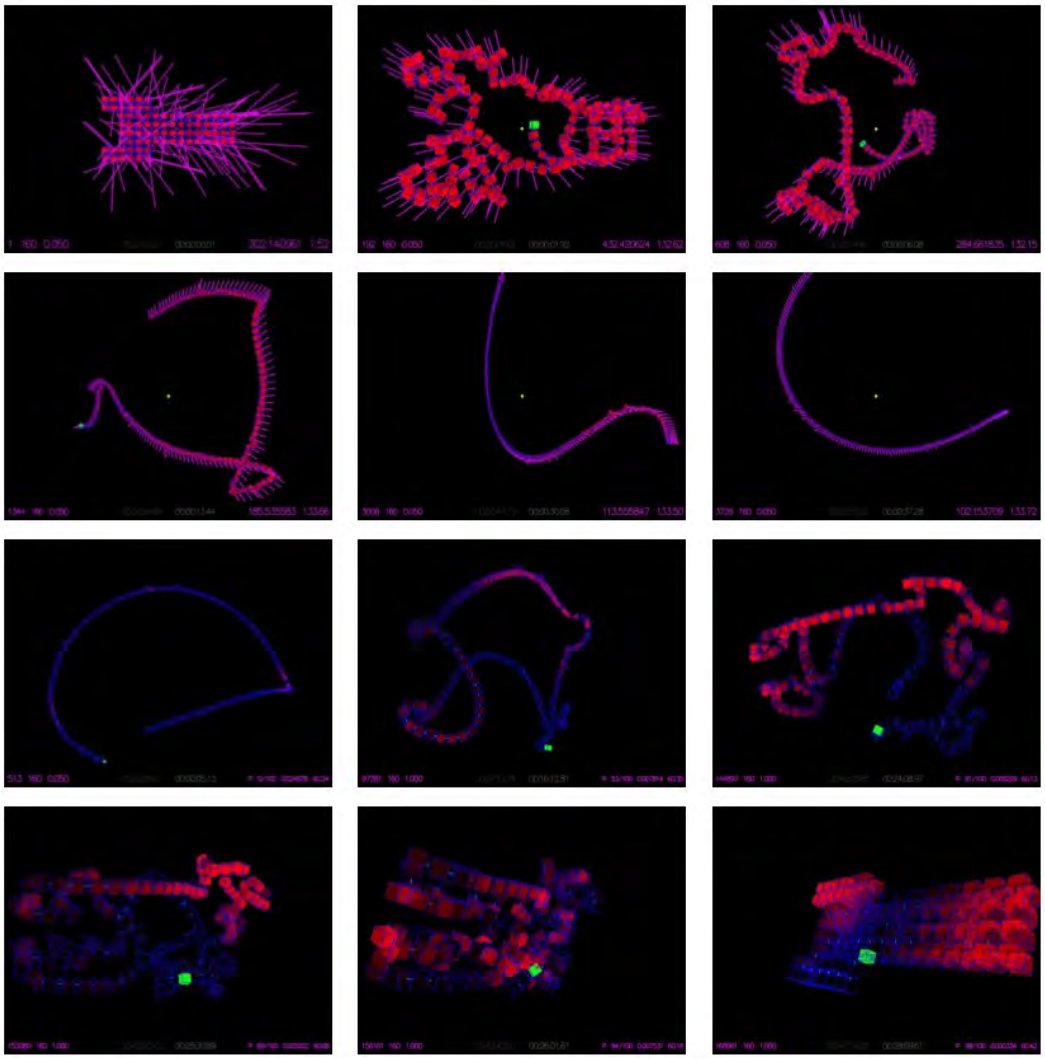

Planning the folding trajectory: First, a pre-folded target shape of 160 chained cubes is subjected to the radial explosion forces applied from its center-of-mass outwards. While the chain unfolds, multiple successive snapshots of all joint angles are recorded over time. Next, the joint actuators are servoed to the recorded angle snapshots in the reversed sequence. As a result, the chain folds into the target shape. The top six pictures show the explosion and bottom six show the playback with brightness of red color denoting normalized amount of joint error.

Panelization

We developed an algorithm for generating Hilbert curves for non-uniform shapes. We do this by merging together uniform Hilbert curves generated within an oct-tree decomposition of space. This algorithm can be thought of as a hierarchical curve that can be folded locally and in parallel bottom-up with reduced possibility for intersections.

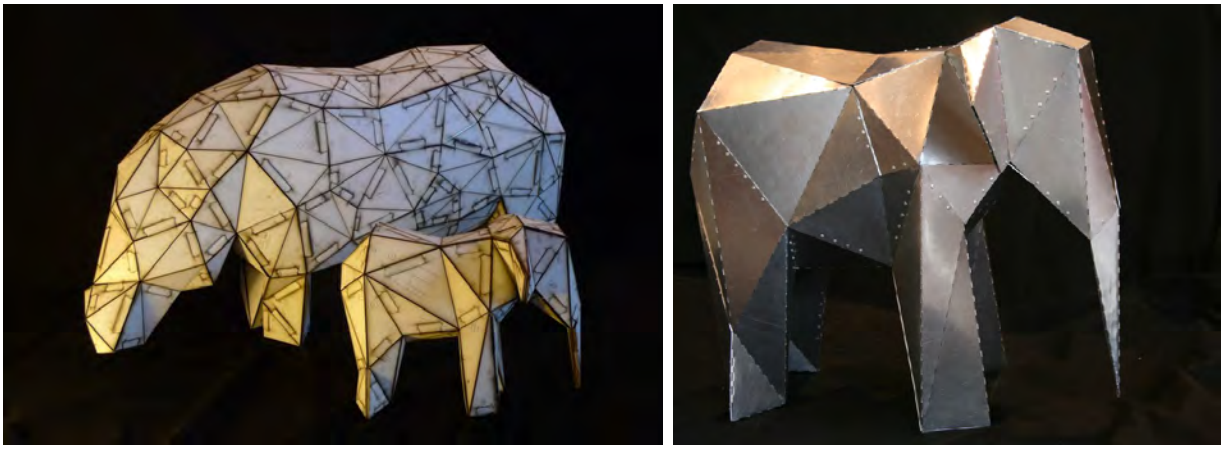

Planar folding of 3D models.

Moteins

We constructed several hardware prototypes of mechanical motorized proteins, from the 200 cm module-pitch mega-motein down to the 1 cm module-pitch milli-motein.

The motein geometry and continuously-connected chain topology has a number of advantages as compared to other concepts for hardware realization of programmable matter. The chain topology means that there is only one (rotary) degree of freedom per element, so it is simple to measure, describe, and control the system. The chain topology makes it easy to pass power and data down the chain, via wired interconnect, without the need for autonomously-operable electrical connectors or local energy storage. The chain provides intrinsic strength in tension, and the opportunity to gain strength in other directions by interlocking or knotting. Finally, the chain allows for actuators in multiple nodes to work together to achieve higher speeds or lift larger loads than is possible with a single actuator.

However, there are some limitations of the chain geometry as well. In the case of lifting a cantilever of nodes, the torque required of each individual node increases as the cantilever gets longer, and there is some maximum number of nodes that can be lifted as a cantilever given a module torque limit. A permanently connected chain is not robust to certain types of individual module failures. For example, if the communications link fails in a node, nodes on either side cannot communicate with each other anymore, potentially incapacitating the entire system. To produce a large

object with thousands of modules, a very long chain will be required, much longer than the spatial extent of the final object. There may not be room for the chain to unfold into a straight line, necessitating more complicated procedures for reconfiguration.

Direct-Drive Milli-Motein

The milli-motein is a chain of programmable matter with a 1 cm axis-to-axis pitch. It is an interlocked series of connected motor rotors and stators, wrapped with a continuous flex circuit to provide communications, control, and power transmission capabilities. The design is highly integrated, with a small number of parts serving multiple functions. The milli-motein uses the hexagonally-bisected cube folding geometry, so a long-enough chain can fold itself into a digitized representation of an arbitrary geometric shape.

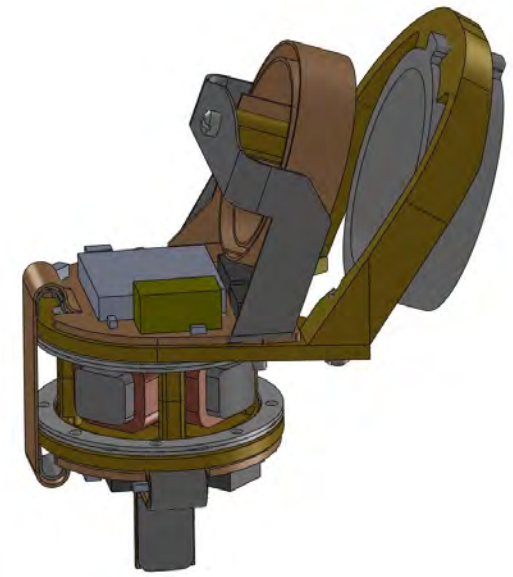

Milli-motein module. This assembly is repeated for each joint. The stator on this module mates with the rotor on the adjacent module.

In designing the milli-motein, we aimed to meet the 1 cm mesoparticle size target specified in the Programmable Matter BAA. We found that it was possible to use off-the-shelf electronics components and fasteners. However, we were not able to find a suitable off-the-shelf rotary drive with the required torque, power, and small size. This led us to invent a new type of motor, the electropermanent stepper motor, which provides high-torque (1 N-mm) drive at low RPM (1-10 RPM) without gearing, and static holding without power.

Design Overview

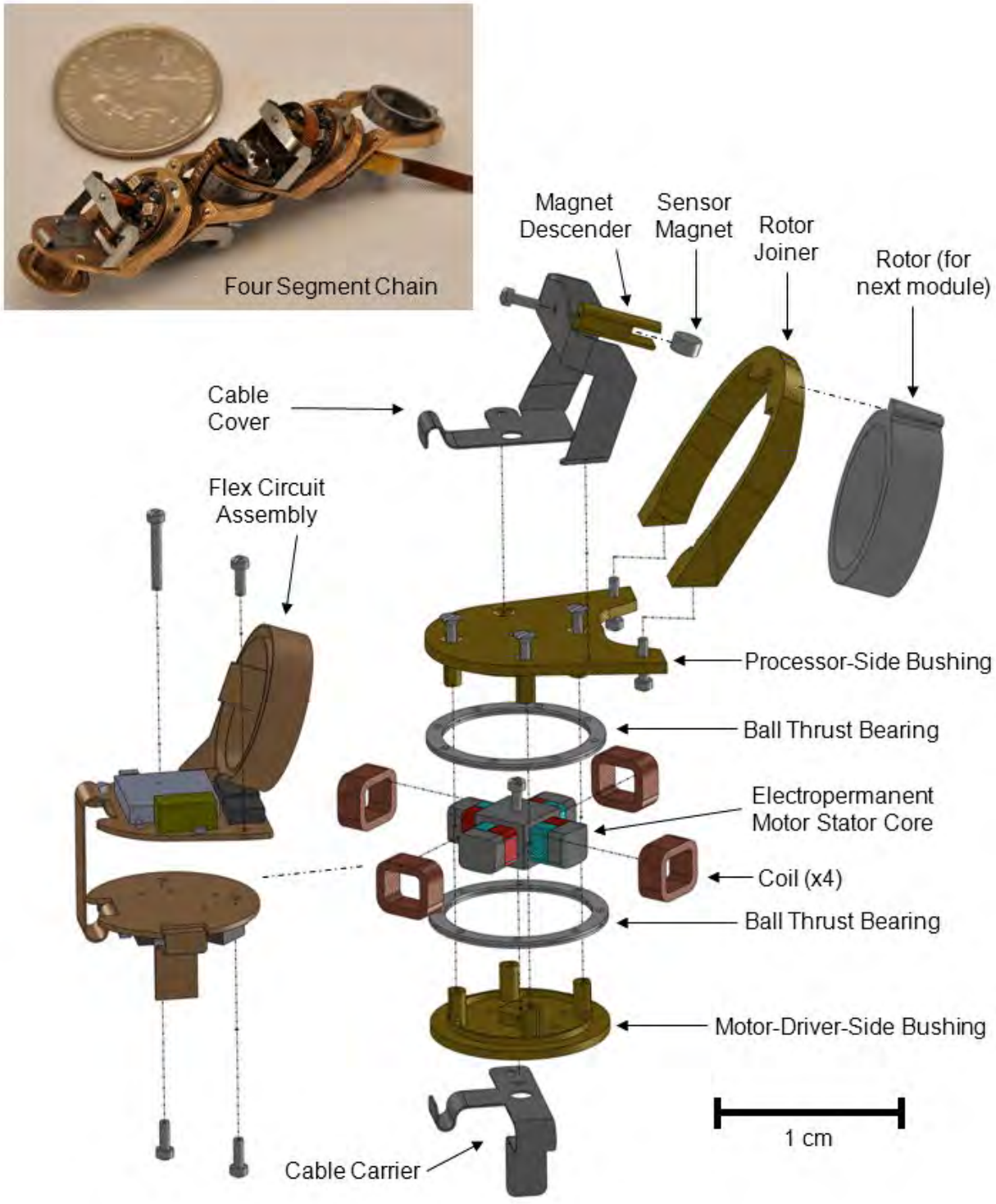

Milli-Motein Module Exploded View. This assembly is repeated for each joint. One segment of the continuous flex circuit is shown in its folded configuration. The stator on this module mates with the rotor on the adjacent module.

The flex circuit that wraps around the chain has two alternating circuit boards, so that the motor for each module is sandwiched between one board of each type. The processor board contains an 8-bit microcontroller, a bank of capacitors to store the energy required for one motor pulse, and one of three half-bridge motor drivers. The motor driver board contains the other two half-bridge motor drivers, as well as the two-axis magnetoresistive position sensor. Each processor has two serial data communication ports, which are connected in a daisy-chain configuration. Power is bussed along the chain.

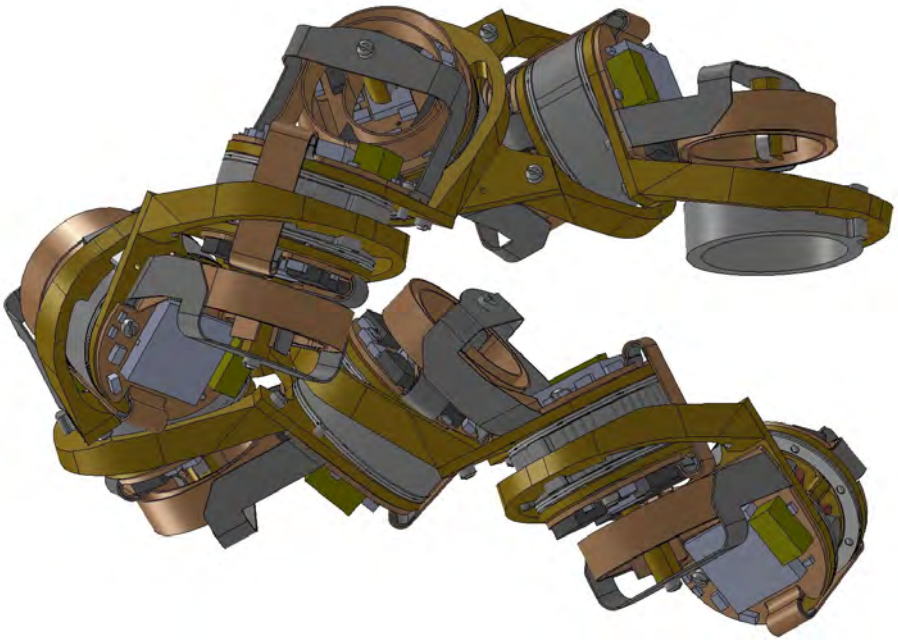

Milli-motein chain, assembled by interlocking milli-motein modules and wrapping the flex circuit. When the chain is assembled, the rotor of one module surrounds the stator of the next, and the sensor magnet of one module is positioned above the magnetoresistive rotation sensor of the next module. Power and data are transferred between modules by a coiled section of the flex circuit. The diameter of the coil expands and contracts as the joint rotates.

Each module is built around an electropermanent stepper motor. The stator is made or Iron, NIB, and Alnico 5. The pieces are cut to size by wire EDM, cleaned, and glued together with epoxy. We then wind a coil around each arm of the stator, and set the bond-coat of the wire to keep the coil from unraveling. When the chain is assembled the rotor from the next unit goes around the stator. The rotor is an iron ring, made by milling. The rotor inner diameter is 75 micron larger than the outer diameter to permit the wobble motor action.

The rotor is constrained axially by two ball thrust bearings, which are sandwiched between the motor-driver-side and processor-side bushings. They allow the rotor to

freely rotate, and to move radially and tangentially over a limited range, but do not allow axial motion. The ball thrust bearings consist of eight 500 um diameter stainless steel balls, held in an evenly-spaced circular pattern by a bronze ball retainer. The top and bottom halves of the ball retainers are made by milling, the balls are inserted with tweezers, and then the ball retainers are soldered together to retain the balls.

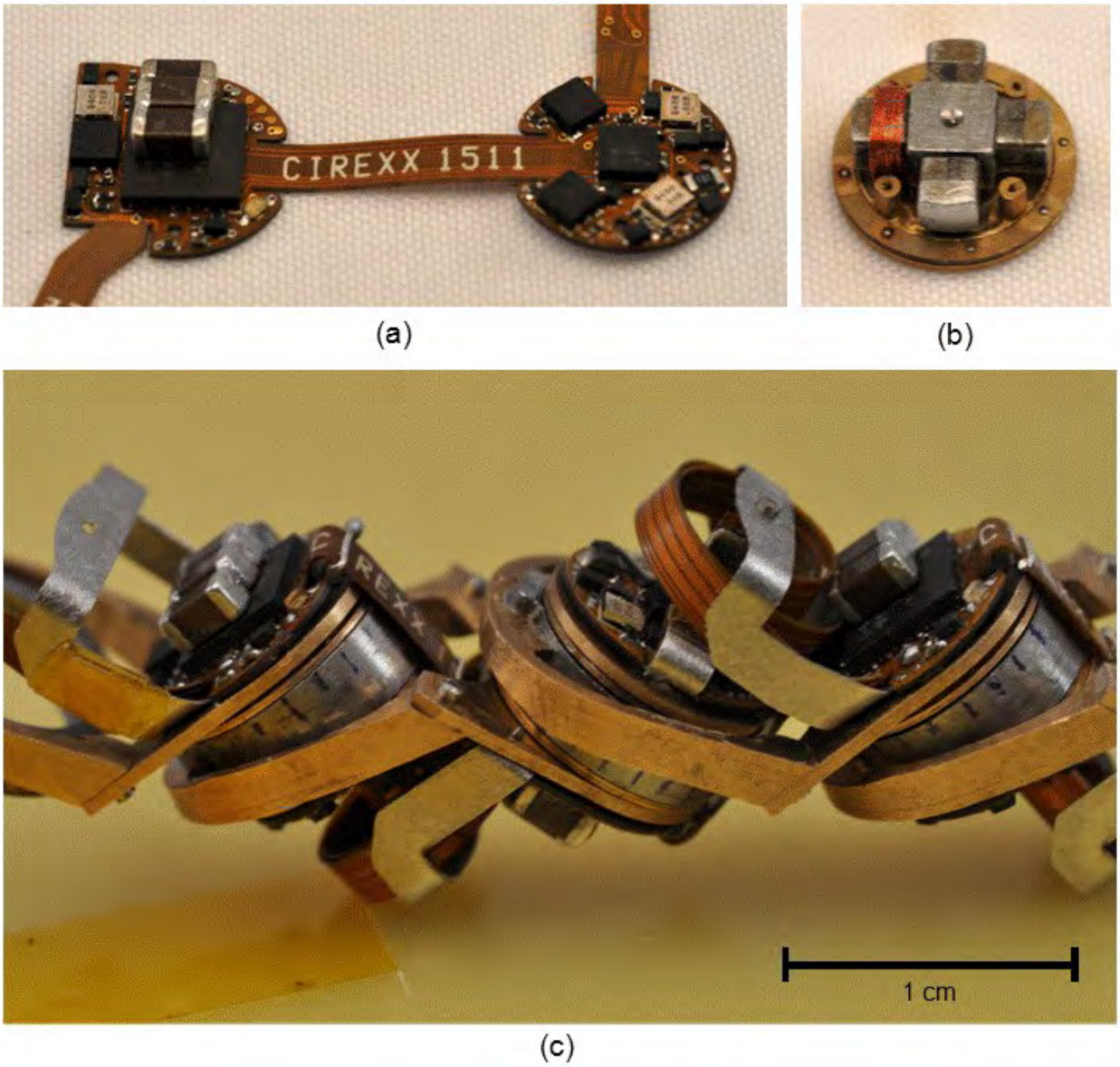

(a) The repeating section of the milli-motein flex circuit. The processor board (left) contains an 8-bit microcontroller, a capacitor bank to store pulse power for the actuator, and one of the three half-bridge motor drivers. The motor driver board (right) contains the other two half-brige motor drivers and two-axis magnetoresistive sensor at the center. (b) Partially assembled electropermanent motor. Only one of the four coils are installed in this photo. The stator core and the tips of the stator arms are made of iron. Each arm is interrupted by a parallel pair of NdFeB and Alnico magnets,

forming a switchable electropermanent magnet. A ball thrust bearing and motor-driver-side bushing are also visible in this photo. (c) Fully assembled milli-motein.

The motor-driver-side and processor-side bushings are major structural components of the module. The electropermanent motor stator core is fastened to a pedestal at the center of the motor-driver-side bushing using a screw. The motor wires are routed through holes in the bushing, surrounded by 500 micron diameter medical teflon tubing to protect them from damage. After the rotor and ball thrust beaings are inserted over the stator, the processor bushing is screwed on to the other side, forming a closed package. The motor-driver bushing and processor-bushing have integrated standoffs so that they can attach firmly to one another and leave about 50 micron of axial play in the rotor when the stack is assembled.

The flex circuit assembly attaches with screws to the bushings on each side of the motors. The motor wires protrude through unplated holes on the motor driver board and are soldered to adjacent SMT pads. The module connects to the next module though the rotor joiner, a bracket that screws to the processor bushing of one module and is soldered to the rotor of the next module. The rotor joiner creates the 109.57 degree angle between adjacent modules that is required for the hexagonally-bisected cube geometry.

A coiled section in the flex circuit allows it to transition between modules. As the modules rotate, the coil expands and contracts. The cable carrier and cable cover are made from 125 micron-thick folded stainless steel. They act to constrain the flex circuit so that it moves in the intended way. The cable carrier holds a flex circuit tab upright near the center of the module, to keep the coil from falling over. The cable cover keeps the coil constrained axially, to prevent tangling.

A cylindrical permanent magnet is mounted from the cable cover, so that it sits above the two-axis magnetoresistive sensor of the adjacent module. Together, they form a rotary position sensor that allows the module to measure its angle with respect to the previous module, to allow for position control and shape reconfiguration.

The Electropermanent Stepper Motor

The electropermanent stepper motor stator is cross-shaped, with an outer circular pole. The rotor has a slightly larger inner diameter, and rolls around the stator in an eccentric pattern combining oscillating translation and continuous rotation. The rotor, stator core, and stator tips are made from soft magnetic iron. Alnico and NIB permanent magnets are placed in parallel at the center of each arm of the stator. An insulated copper wire coil is wrapped around each arm, which is used to switch the magnetization of its Alnico magnet. The NIB magnet in each arm has a high coercivity, so its magnetization is not substantially changed by current through the coils. Thus, each arm of the stator is an electropermanent magnet.

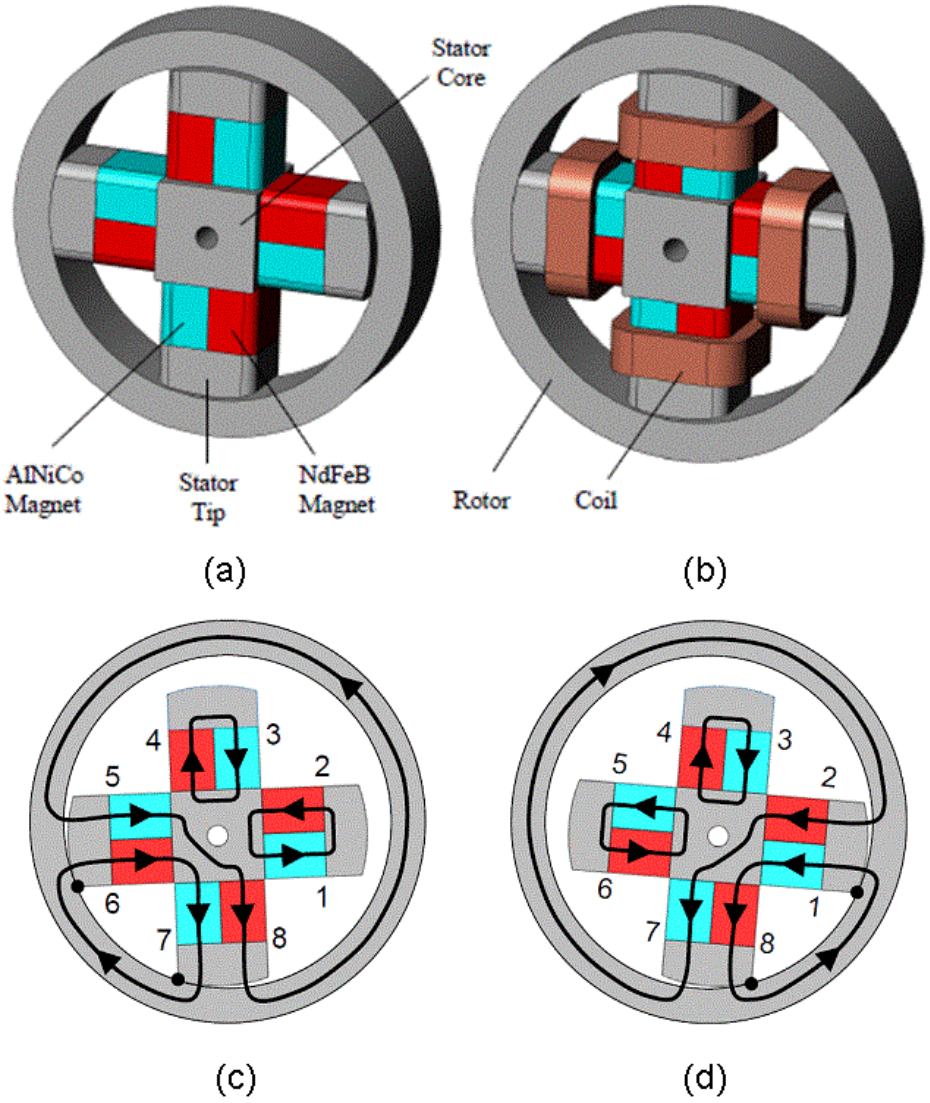

Electropermanent stepper motor. The red magnets are NIB, always polarized in the direction shown. The magnetization of the blue Alnico magnets switches as the motor operates. The motor starts in position (c), with magnets 5-6 and 7-8 on, and magnets 1-2 and 3-4 off. Flux flows through the rotor and stator as shown. Applying a current pulse to the horizontal winding around magnets 5-6 and 2-1 switches the magnetization of magnets 5 and 1, turning magnet 5-6 off and magnet 2-1 on, resulting in the new flux paths shown at right. The rotor pivots counterclockwise about magnet 7-8, taking one step to arrive at the new position shown in (d). Repeated steps drives the rotor around the stator with a continuous rotary motion and oscillating translational motion.

In the initial condition, two adjacent magnets are switched on, causing the rotor to adhere to their ends by friction. A pulse simultaneously turns off one magnet and turns on the opposing magnet. The rotor rolls along the perpendicular magnet, which stays on continuously, moving away from the magnet that switched off and toward the

magnet that switched on. Repetition of this sequence results in continuous rotation with superimposed vibration. The NIB permanent magnets are placed with alternating magnetization direction around the stator, so that when adjacent arms are switched on, there can be a loop of flux through the two arms and the rotor. Because the coils on opposite arms are always used together, they are continuously wound, so that the device has two electrical phases.

Assembly

Assembling the milli-motein proved to be a challenging manual operation. We manipulated the parts using titanium tweezers under a stereo microscope, and joined them by soldering, using epoxy, or fastening using 0000-160 (500 micron diameter) screws. Our approach to assembly was to extend the family of techniques used for electronics assembly at this scale to assemble the mechanical parts of the system as well. We used soldering to join metal parts, epoxy to join the heat-sensitive permanent magnets, and screws to reversibly fasten subassemblies that might require subsequent removal for repair. Due to the small size of the parts, a significant portion of the time for assembly was devoted to scraping and cleaning procedures, to remove grease, waxy deposits, fibrous materials, corrosion, dirt, and EDM scale from the parts to prepare them for assembly.

The small size of the parts relative to our tools made them fragile -- not during actual operation of the robotic system -- but during assembly and especially repair. During assembly, ripping or kinking of the flex circuit, failure of epoxied joints, nicking of magnet wire insulation, knocking components off the board, and stripping of threaded fasteners were not uncommon occurrences. To compound matters, a relatively small mechanical defect (such as a nicked wire) could then lead to a serious and systemic electrical fault -- requiring major repair work that could then lead to additional mechanical damage. Through design revisions to facilitate assembly, carefully planning and documenting the assembly procedure, and increasing mechanical skill, we were able to construct working prototypes.

Software

Each processor runs identical firmware, a command monitor that processes commands and issues responses. A program running on a PC provides high-level control of shape reconfiguration, sending commands down the serial chain connecting the processors.

Upon power-up, the PC sends the “discover” command, which is passed down the chain with an incrementing number, allowing each chain to discover its ID. Thereafter, the PC can select individual nodes and read or write their registers. In doing so, the PC can read the current angle, set a desired angle, and initiate motion.

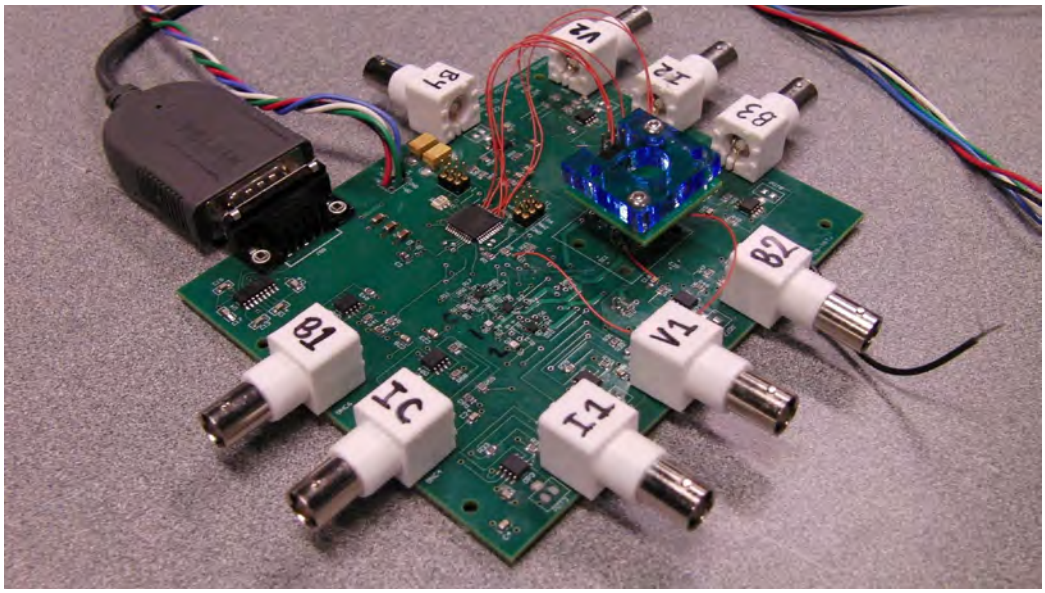

Milli-motein development node.

The geometry of the chain is fully described by its vector of joint angles. The output of the folding workflow is a sequence of joint angle vectors that define a path through configuration space for the chain to take to reconfigure from one shape to another. During shape reconfiguration, the PC loads each node with its desired angle, initiates motion of all nodes simultaneously, waits for completion, and then repeats for each step in the reconfiguration sequence, until the desired endpoint geometry is achieved.

Motor Unit Testing

Electropermanent stepper torque *vs* speed curves were measured by hanging weights on a string from the rotor, and recording the time for one revolution with a stopwatch. Excitation was with 30V, 60us pulses, spaced apart either 4 ms or 40ms.

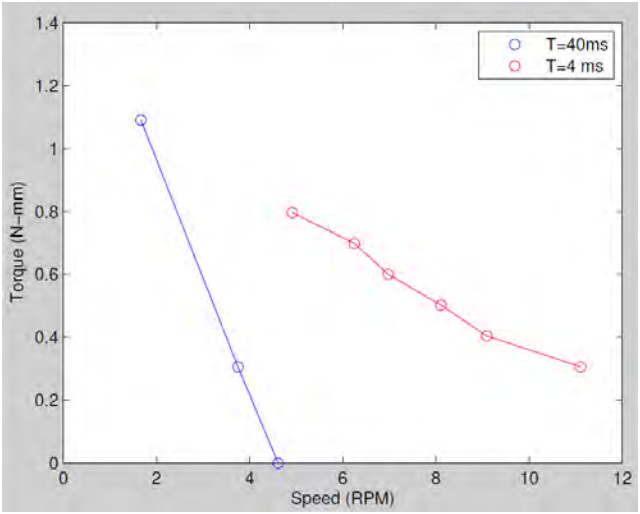

Electropermanent wobble stepper motor torque/speed curve.

The motor efficiency was compared to existing micro-motors, showing the unique high torque at low RPM.

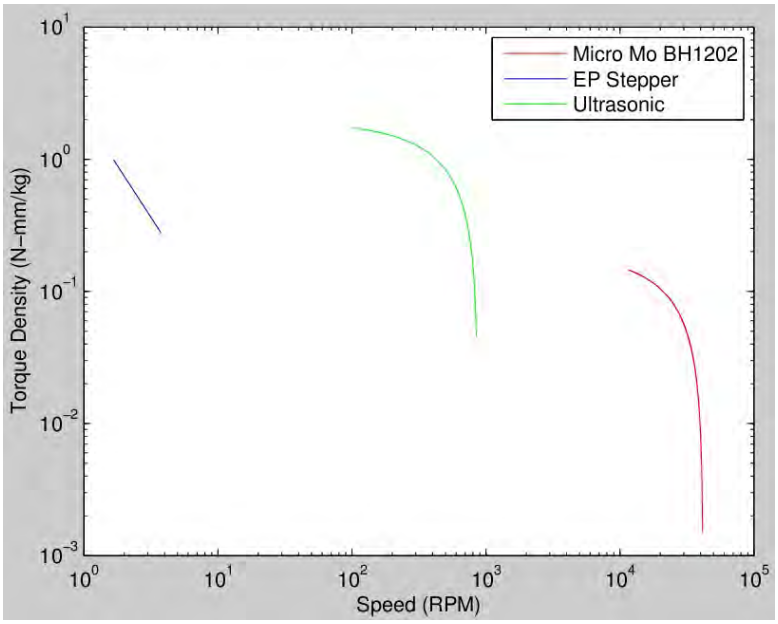

Electropermanent stepper motor efficiency.

Shape Reconfiguration Testing

We placed a four-segment milli-motein on an FR-4 platform, with power supplied a bench power supply and a serial link from the first node. The operator could command the motein to change between shapes.

The chain drew 35 mA on the 5V rail continuously, to power the processor and sensors, and about 100 mA on the 29 V rail during shape reconfiguration, to power three motors operating simultaneously. Shape reconfiguration time through 90 degrees was about 5 seconds. The motor step pulse length was 60us, and the pulse-to-pulse time was 10 ms, with eight pulses per step cycle.

The mass of each segment was 3.5 grams. With the chain extended in a straight horizontal line, a single node was able to hold the weight of the other three nodes without its rotor slipping. Nodes were able to actively lift a one-node cantilever through the maximum-torque horizontal position, but barely not able to lift a two-node cantilever (attempting to lift a two-node cantilever resulted in very slow backward motion).

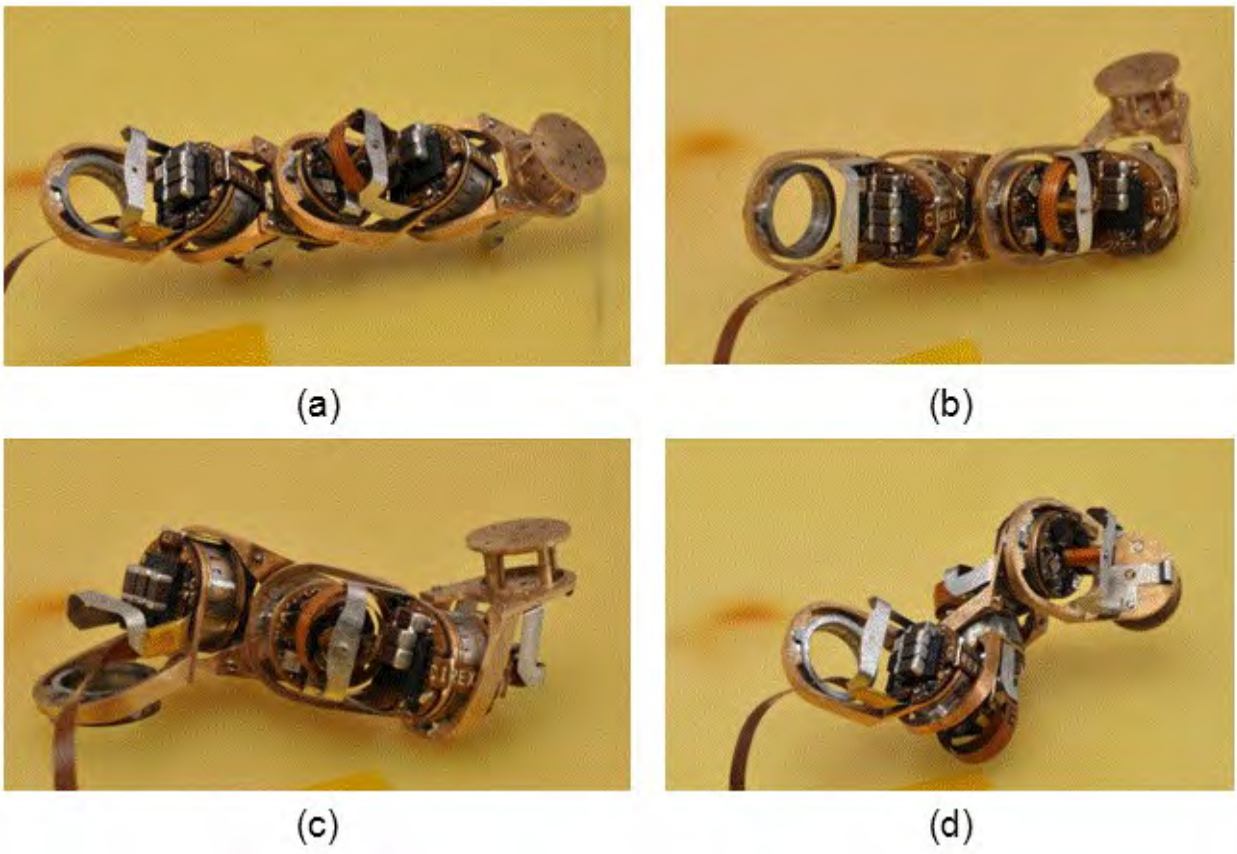

Four-segment Milli-Motein rendering four geometic shapes. (a) straight line [0 0 0] (b) L-shape [0 0 90] (c) periscope [-90 0 90] (d) helix. [90 90 90].

The distance from the center of rotation of the motor to the center of mass of the node it lifts is 13 mm. Based on this, it should take 0.45 N-mm torque to lift a one-node cantilever, and 1.34 N-mm torque to lift a two-node cantilever. This is above the maximum forward torque of the motor, so this is a consistent result.

The milli-motein was able to move itself around on the table, so it seems likely that a battery-powered milli-motein could move itself across a table. The milli-motein was also able to reconfigure from a stable shape to an unstable shape which would then fall over, which could be used for locomotion.

It was possible to switch the chain from a straight line to any of the four shapes shown above and back to a straight line simply by commanding all nodes to go to the desired angle at once, without any motion planning. However, even with this fairly short chain, motion planning would have allowed for a greater variety of shapes to be formed. Sequencing of the moves to lift up certain parts of the chain before others, it was possible to reach configurations that could not be reached by simply driving all actuators toward the target at once, because in this case the chain would wedge itself against the table. The same configuration (e.g. a straight line) has multiple stable orientations on the table, so some information about the overall orientation of the chain

(perhaps from a single two-axis accelerometer at one end of the chain) would be needed in order to do gravity and torque-aware motion planning.

Feasibility of Building a Longer Chain

With the design fully worked out, it took about six man-hours of assembly, about two hours of unattended CNC mill and EDM time, $12 in electronic components, a flexible circuit board, and a negligible amount of raw materials and shop consumables to build each node. With manual assembly, labor costs would dominate; at $30/hr for assembly labor and $50/hr for machine shop time, we get a cost of about $200/node at medium volume, plus setup time and tooling. This puts the cost of labor and materials to build 100 cc of programmable matter using the design shown here at $20,000.

Before this was undertaken, through, there are a few design changes that would be advisable:

- The circuit should be equipped with protection components so that it is robust to arbitrary electrical fault conditions on the interface connecting the nodes. Because the circuit board layout is very tight, this might require a small increase in the module size.
- A plastic shell should be designed to cover the circuitry of each node, to protect it during final assembly of the chain.
- The ratio of torque to module weight should be increased so that each module can lift the weight of two modules instead of one. An easy way to do this would be to use aluminium instead of bronze for the structural components, and to use Hiperco-50 instead of iron for the stator tips and rotor.
- Building jigs and fixtures for each step of the assembly, to hold the parts in the exact orientation needed, would dramatically reduce the assembly time required, lowering the per-node cost.

A desktop robotic micro-assembly machine would greatly facilitate projects such as this one, and allow a much greater variety of design options to be tested and produced in a short time. One way to build such a machine would using 2-3 miniature 6 DOF robotic arms with interchangable heads. Heads could include grippers, a screwdrivers, screw holders, a dispenser for glue/sovents/solder, a hot-air soldering pencil. Component parts and subassemblies could be laid out on the table and found/oriented by video. Features could be engineered into the parts to facilitate gripping. CAM software for the assembler could allow planning of the assembly sequence using the assembly CAD data. Such a machine could allow many more design variations to be tried in a short time, resulting in improved designs, and would allow for the production of smaller nodes, yielding higher-resolution prototype programmable matter.

Macro-Moteins

The DeciBot is the largest of the motein family of programmable matter 1D folding chains with overall dimensions of 144”x18”x18” unfolded and 36”x36”x36” when folded into a cube. The unit geometry, similar to the rest of the motein family, utilizes the hexagonally bisected cube connected in a linear chain. The MacroBot is the predecessor to the DeciBot with overall dimensions of 110”x11”x11” unfolded and 22”x22”x22” when folded into a cube. The DeciBot and MacroBot systems contain electromechanical actuation at each node allowing 360 degree rotation and three positions of discrete alignment (-120,0,120). Each node contains hard-wired communication to neighboring nodes, joint angle sensors to detect position and direction of rotation as well as turntable bearings and an aluminum shell. The chains can fold from any 1-dimensional configuration into 2 and 3-dimensional shapes through a sequence of joint angles that are passed through the chain. Each unit communicates down the chain to find its current position, then receives the message of angle sequences, moves to the designated angle with relation to its current position and passes the message to its neighbor. The reconfiguration can be done sequentially or nodes can move simultaneously along the chain.

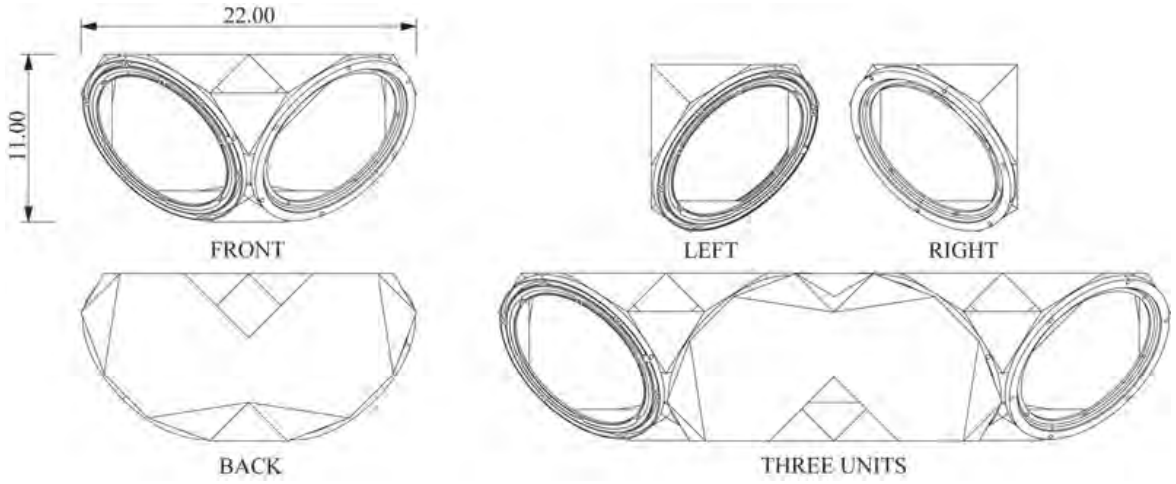

MacroBot: hexagonally-bisected cube geometry and dimensions.

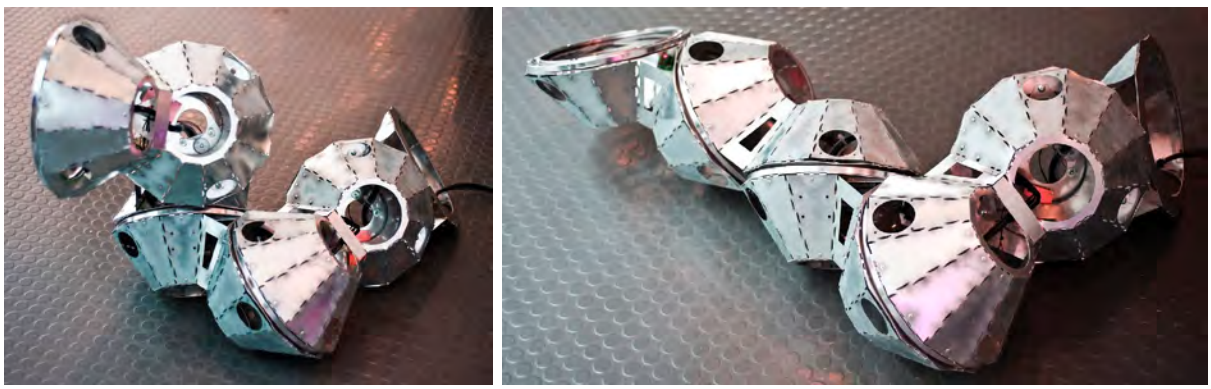

Macrobot chain.

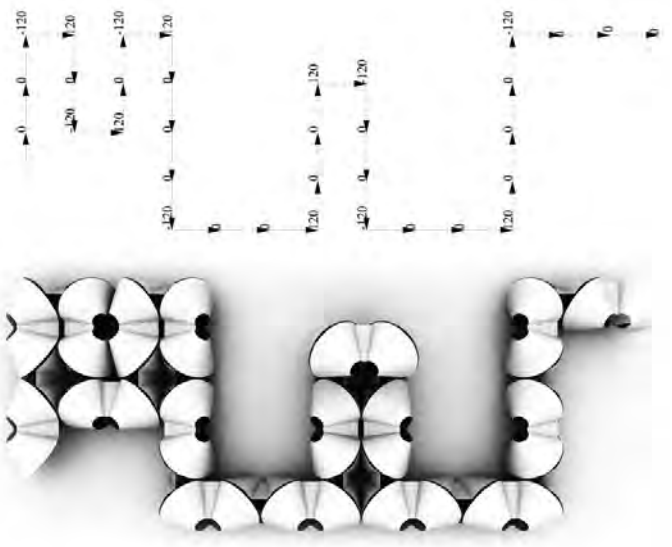

Joint angles to describe the letters "MIT".

Macrobot fold sequence from a line to an arbitrary shape and back to a line.

DeciBot chain.

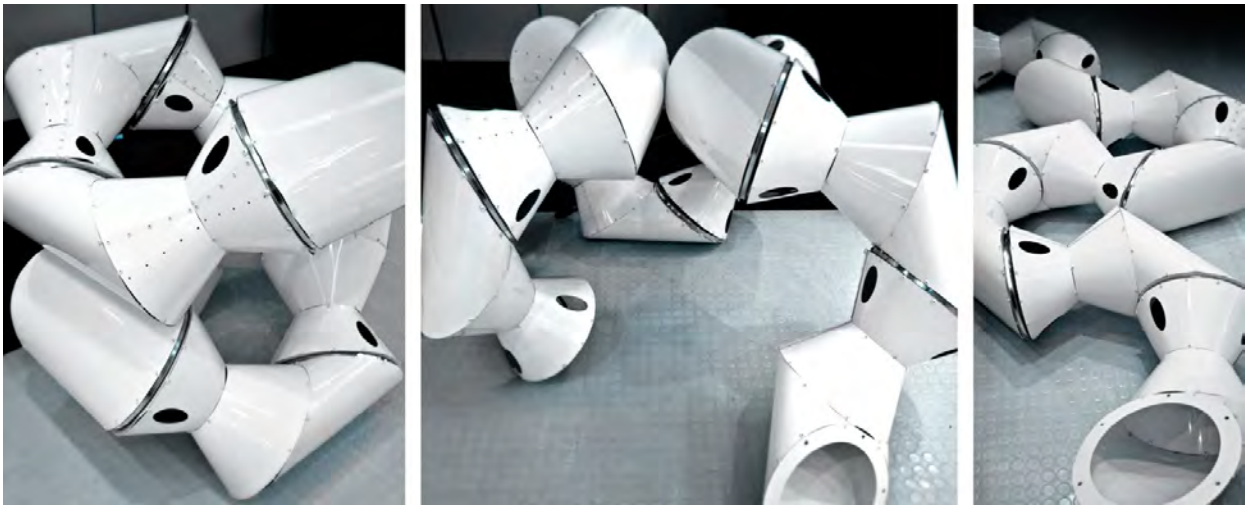

DeciBot chain.

MacroBot & DeciBot internal gear, bearings, and communications.

Macro Passive Folder

The Passive Folder is a subsequent development in the motein family of programmable matter hardware. The Passive Folder also utilizes the hexagonally bisected cube geometry as the underlying structure. This prototype aims to maintain the full functionality of the previous electro-mechanical 1D folding chain prototypes, i.e. 3 locking positions of rotation, full programmability/functionality at every node, the ability to construct any given 1D, 2D or 3D geometry from a single 1D input string. However, this version relies on human actuation for programming (pull & rotate mechanism), to translate between given geometries rather than electromechanical devices. The user reads off the joint angles from a given sequence to fold the desired geometry, rotates each joint and continues along the chain.

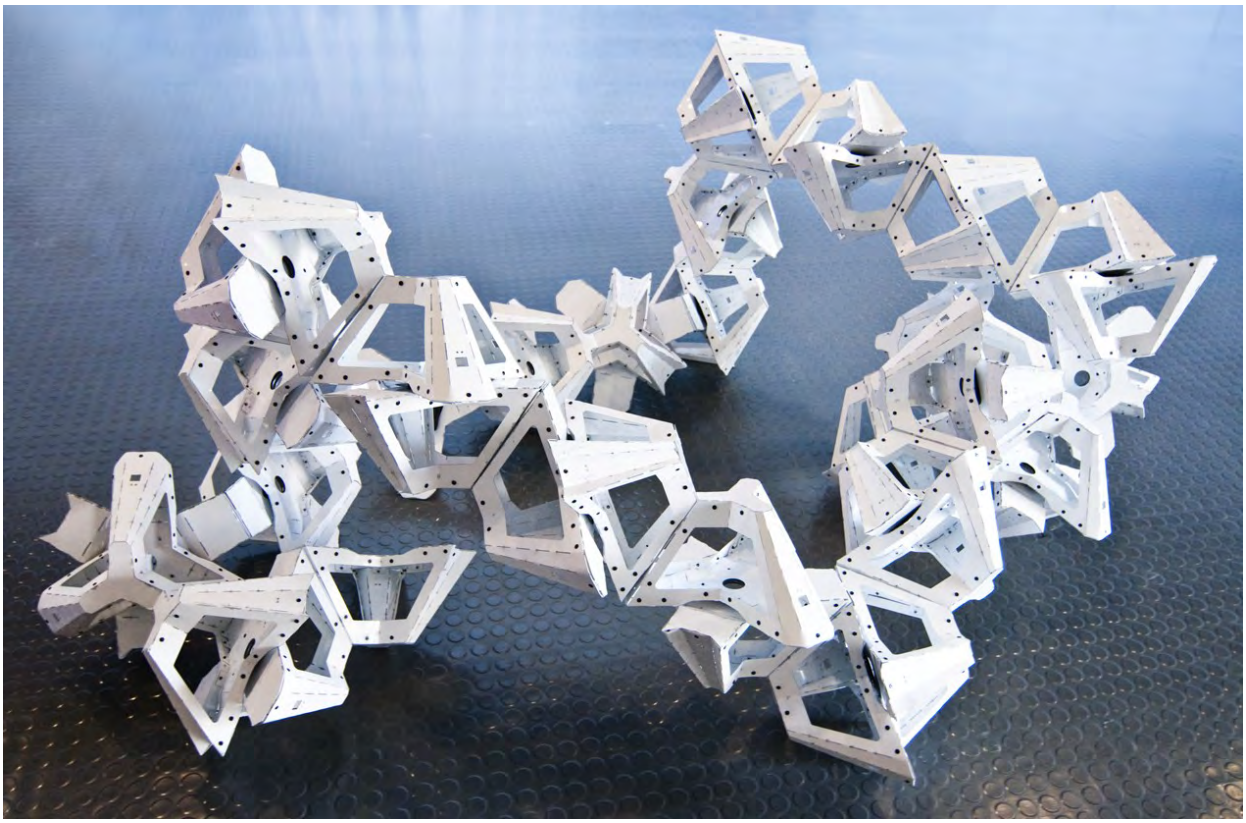

Passive folder chain.

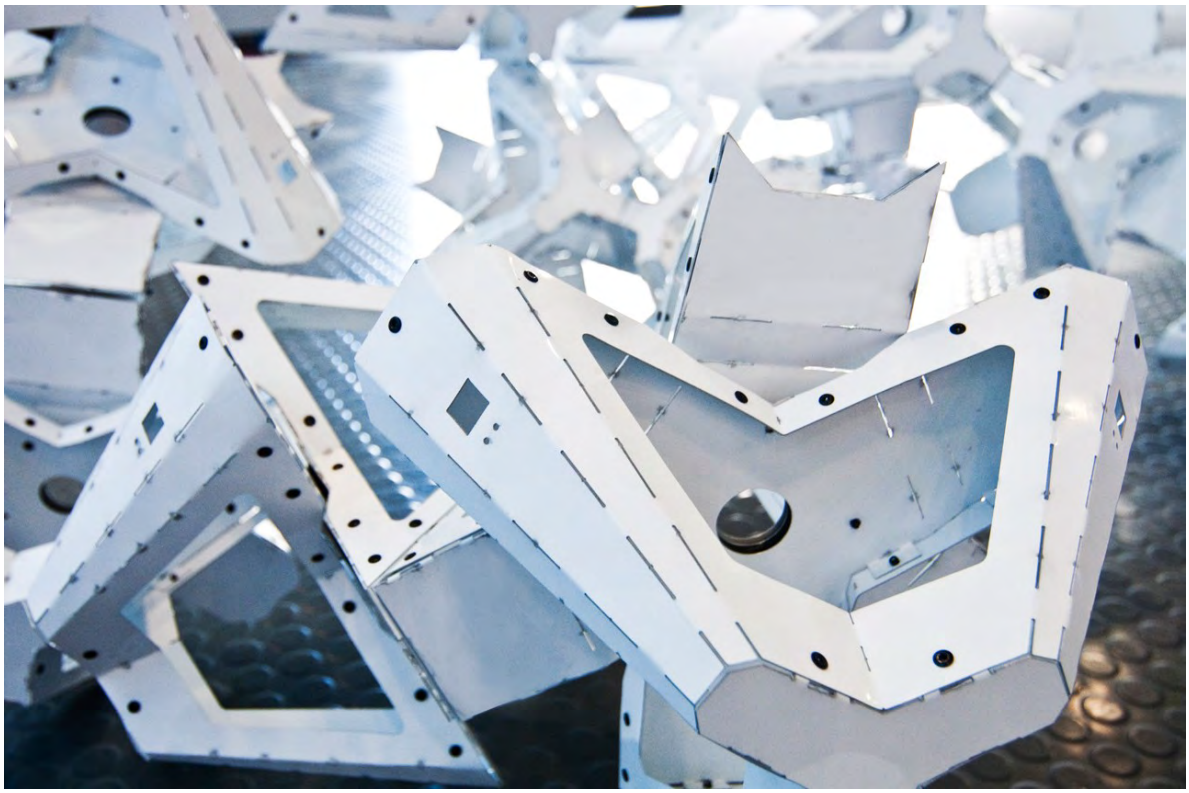

Passive folder unit detail.

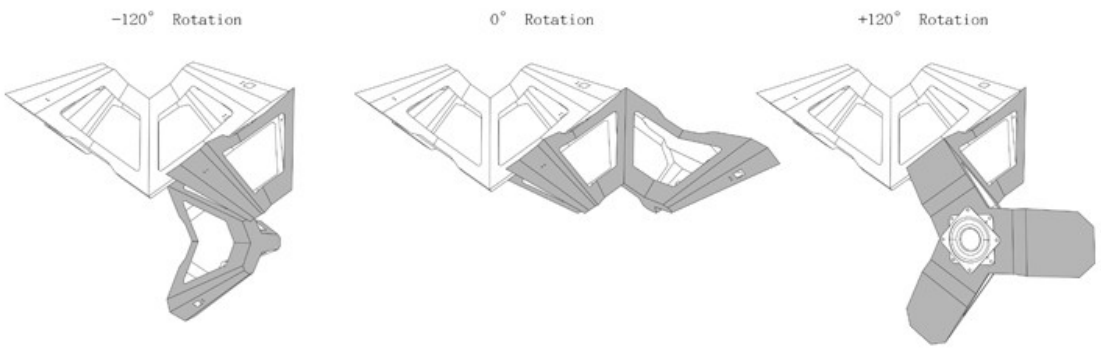

Passive Folder: Three Position Locking Rotation

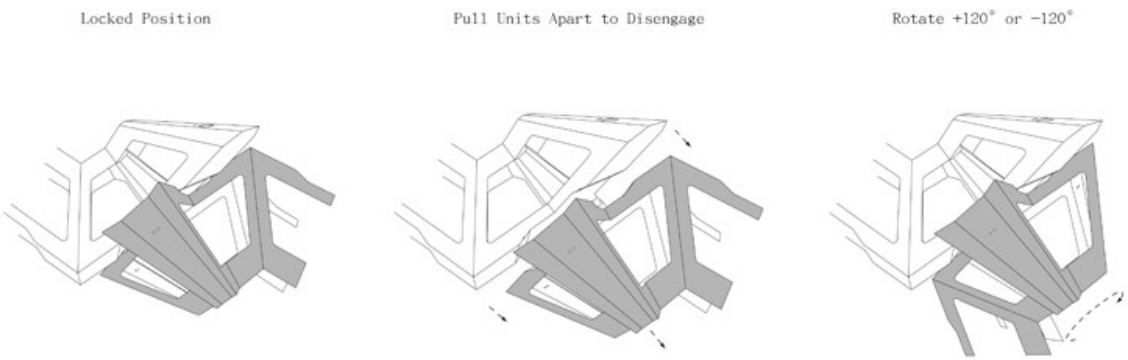

Passive Folder: Female-Female Geometry: Pull & Rotate mechanism

Stochastic Milli-Motein

The goal of this approach is to simplify chain programmable matter by removing the actuator from each node and, instead, put energy into the system externally through stochastic vibrations. Each node takes this random energy input and rectifies it to produce motion towards the target position. We have investigated two variants of this system: 1) smart clutches that can be reprogrammed in situ and fold through arbitrary paths in configuration space and 2) ratchets that are programmed ahead of time and are entirely passive. We developed a chain using the ratchet concept, and identified how the size of the increments of the ratchet, length of the chain, and the amplitude and frequency of agitation affect the folding time and success rate.

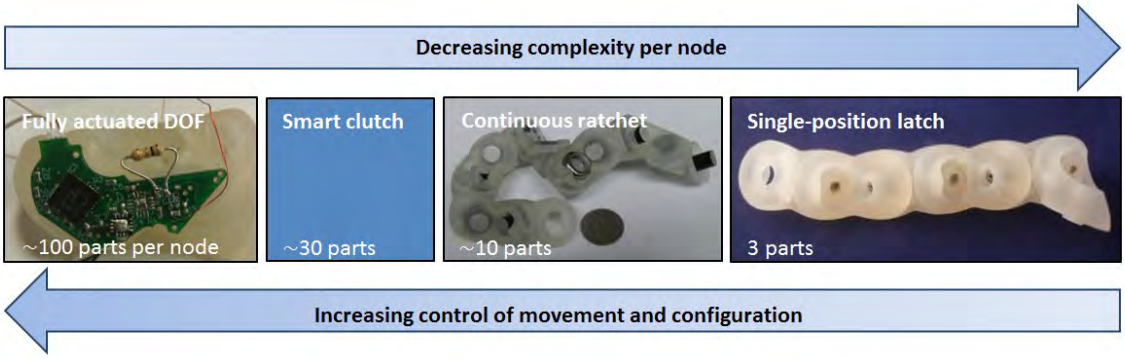

Continuum of controllability and complexity in folding chain systems.

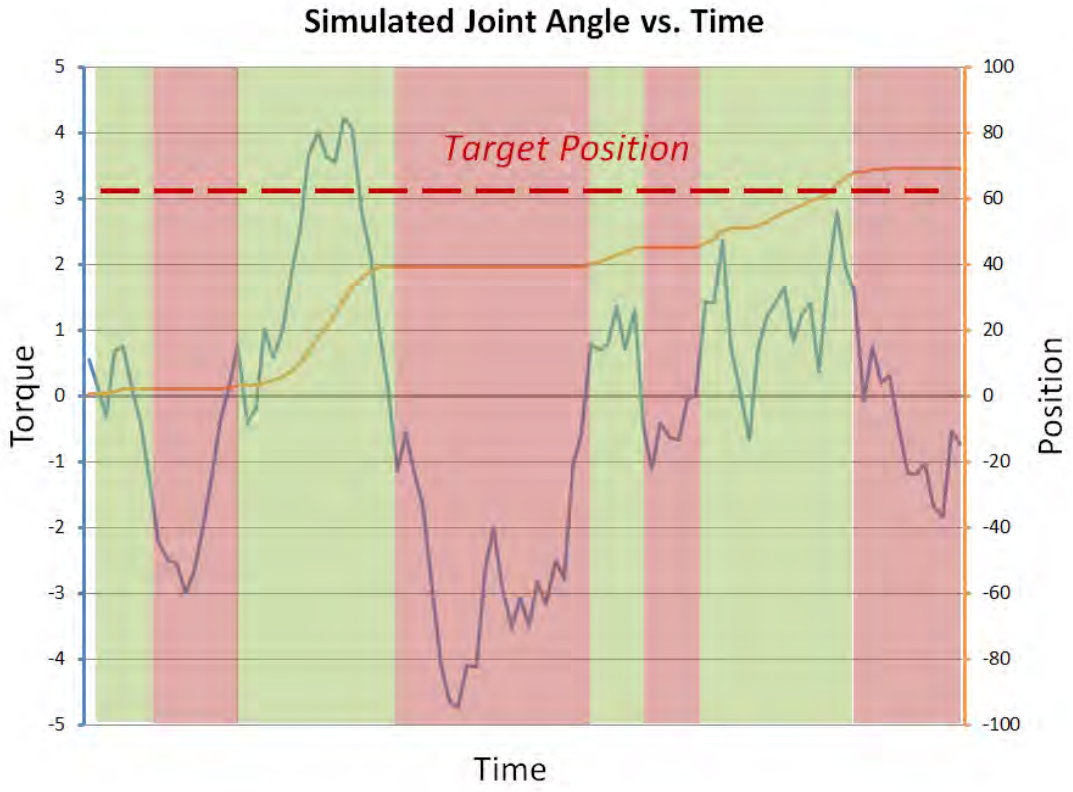

Simulation of random torque applied to a joint and the response of its clutch. The red and green regions indicate when the clutch is closed and when it is open.

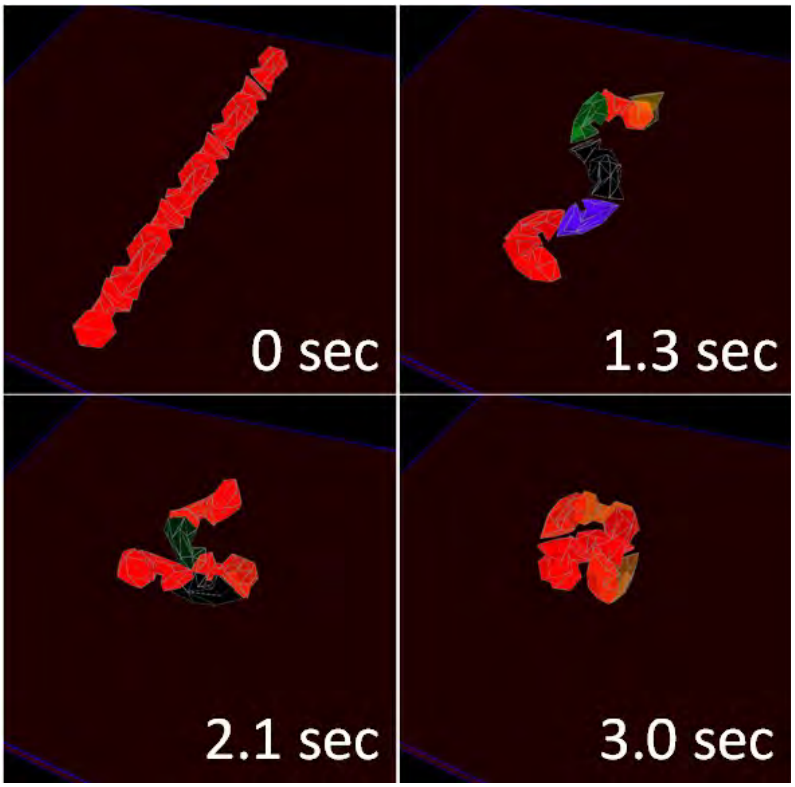

Stochastic folding simulation. The color indicates how far a node is from its target position.

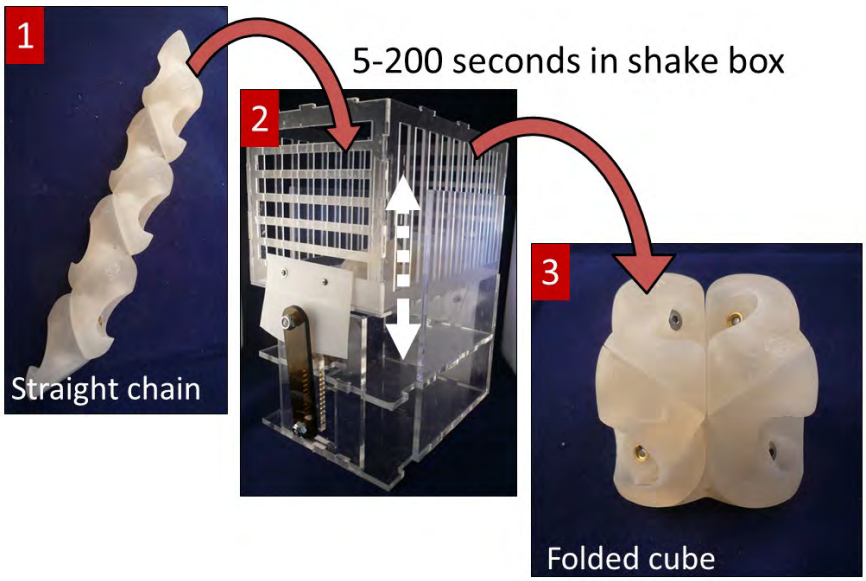

Stochastic folding experiment.

Reconfigurable Asynchronous Logic Automata (RALA)

To program programmable matter we investigated reconfigurability in spatial programming models. This was based on Asynchronous Logic Automata (ALA), which passes state tokens between locally-connected cells on a lattice. There are cell types to perform logic, and to create, destroy, switch, and transport tokens. When a cell has valid tokens at its input and no tokens at its output it pulls the former and pushes the latter. The distance that a token travels is proportional to the time that it takes, the number of operations that can be performed on it, and the amount of information that can be stored. These are all coupled as they are in the underlying physics.

RALA adds a new cell type, a "stem" cell that can convert state tokens into cell configurations. In ALA programs are specified by their shape; RALA allows those shapes to change, to reflect changes in both logic and geometry. Because of its deterministic asynchronous operation, it is possible to "grow" a program that will then turn on self-consistently as local neighborhoods are completed.

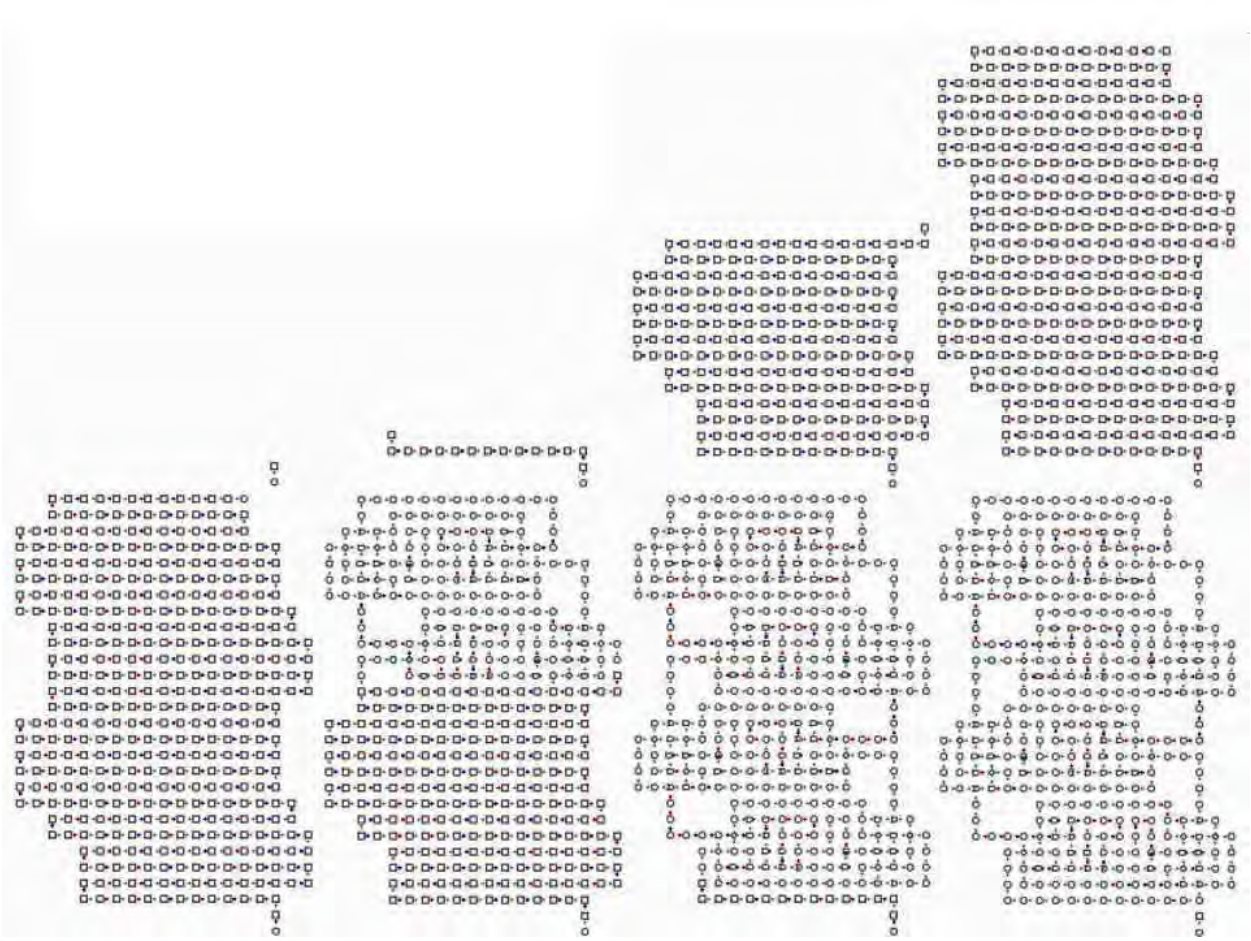

Growth and operation of a RALA sorting network.

With the addition of a stem call, it is possible to implement in RALA staples from the study of self-reproducing systems, such as a replicator loop that copies programs.

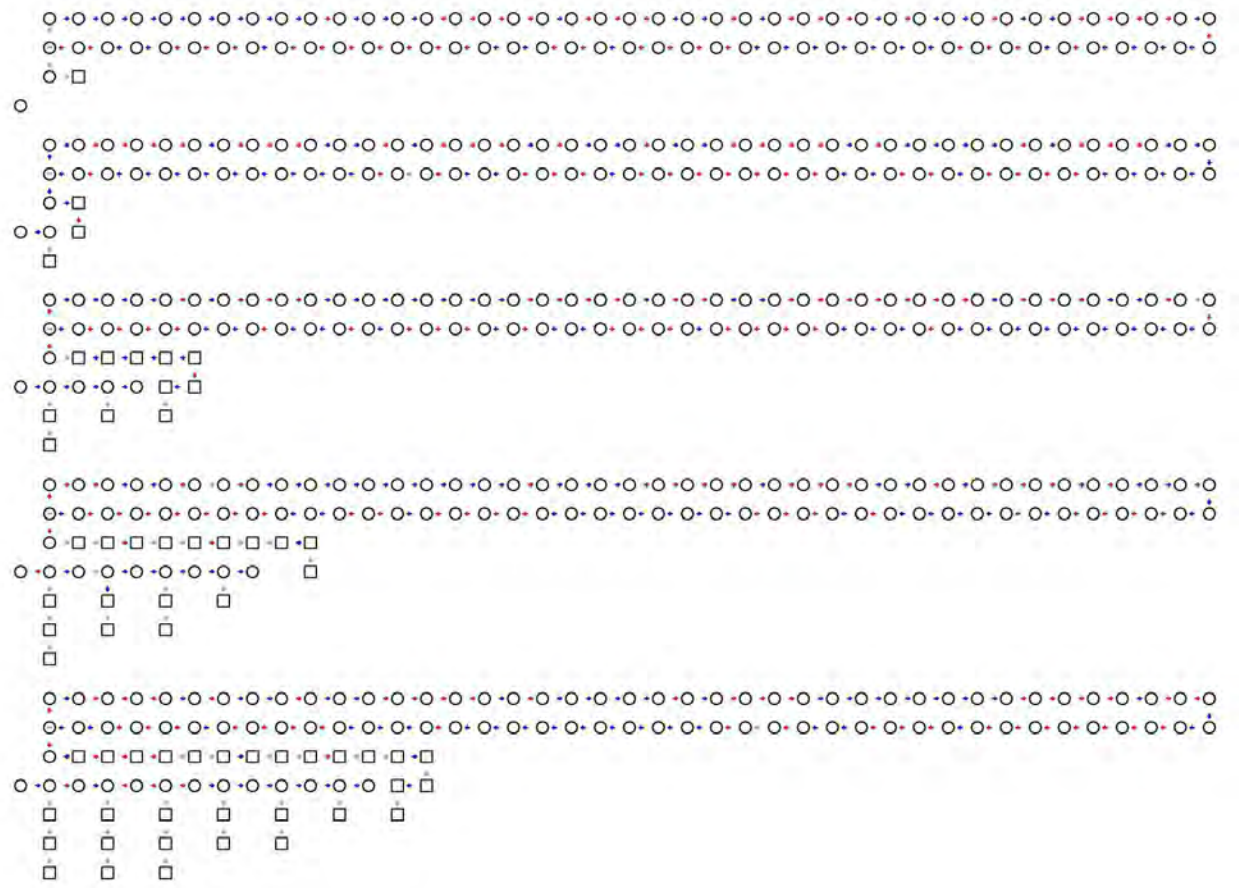

RALA replicator.

To bridge between RALA and programmable matter, a CAD workflow was developed to code for the folding in 2D or 3D of arbitrary shapes. Based on the universality of folding in milli-biology, this provides a unified framework for describing both computation and construction.

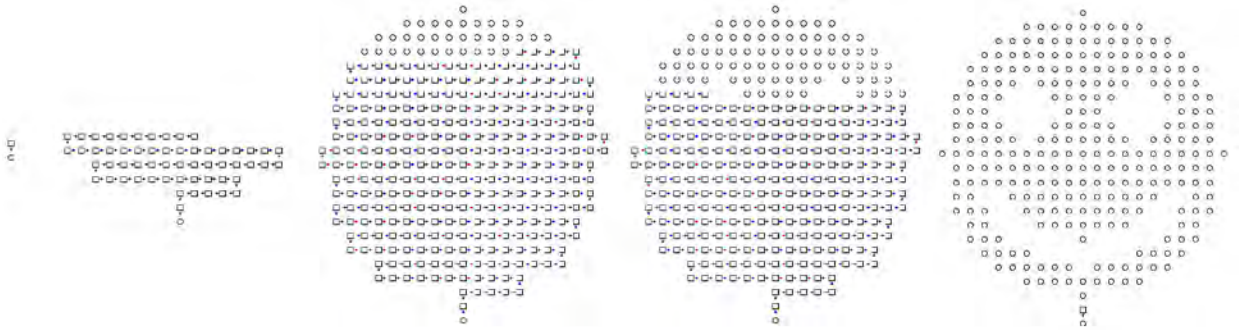

RALA growth of geometry.

Digital Materials

NC machining and 3D printing are computer-controlled, but they continuously add or remove materials -- the materials themselves do not contain information. Compare this with the assembly of a protein: the coordinate system is local to the amino acids rather than imposed globally, errors can be detected and corrected, and bases can be reused. These properties are analogous to those of digital *vs* analog communications and computation.

We call materials constructed from a finite set of parts with discrete local orientations and locations digital materials. Together with an assembler that places them these can be thought of as externally-programmable matter. The combined system of assembler and material is reconfigurable, addressing this goal of programmable matter with significantly simpler parts.

Families of digital material parts were designed that can be assembled vertically (to simplify assembler design) and hierarchically (to span length scales), with reversible mechanical joints. A workflow was developed from a CAD design to an assembly sequence.

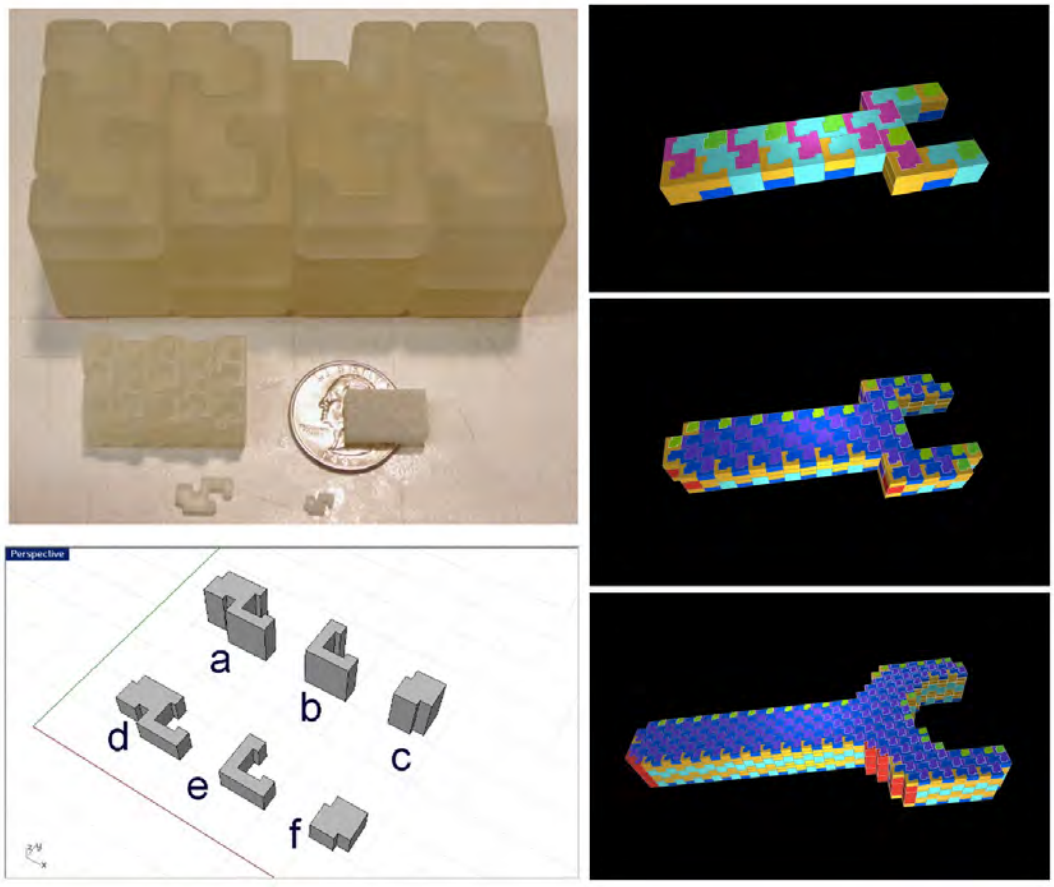

Construction with digital materials.

One of the benefits of digital materials over other approaches to rapid-prototyping is that the components can be constructed from dissimilar materials optimized for an application. An area that was investigated was 3D electronic interconnect, motived by the challenges of the dense design of the milli-motein. Using two-dimensional conducing and insulating tiles, 3D interconnect was demonstrated with arbitrary geometries.

Digital materials for electronic interconnect.

Digital assemblers can be simplified from 3D printers and NC mills because the parts are restricted to lattice locations and can self-align. Preliminary design work was done on assembler designs; unlike existing pick-and-place machines, the restricted part set allows components to be fed directly from the heads.

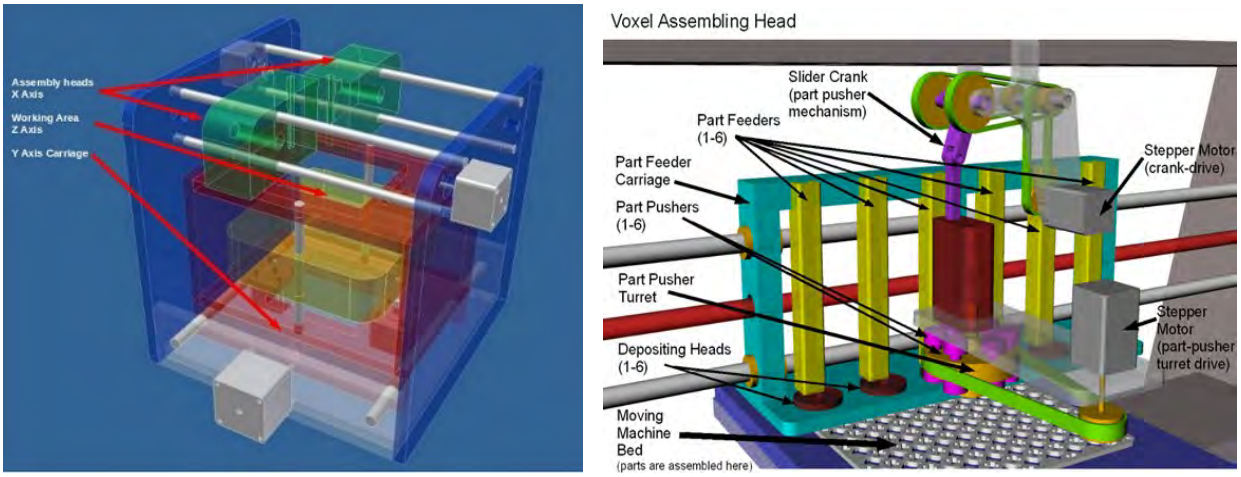

Digital material assemblers.

Microfluidics

We explored several schemes for programmable folding of 1-D chains via self-assembly. Specifically passive fluidic assembly techniques for folding were explored

which have the advantage of scalability (a large number of joints) and affordability (cost per complexity).

Bilayer Thin-Film Folding

DNA-based folding techniques can produce nanostructured programmable objects. The length scale of the driving physics limits the size scale of objects in DNA origami. We have been working on approaches to produce folding structures at nano- and micro-scale using other materials in two areas: curling nanotubes and lipid bilayer tubules. The common principle in both techniques involves using passive dynamics of the systems to allow for folding of structure.

Below we show both schematic design and experimental progress in our efforts to fold programmable tubes from 30-40 nm polymer sheets spin coated on a Si surface. We UV-pattern 2D structures and allow them to curl via expansion due to charging in one polymer layer, resulting in controlled rolling/curling into a tube. Suspended tubes with right (R), left (L) folds lead to folding of programmed structures. The technique can be expanded to 3D folded structures at micron and nanometer scales.

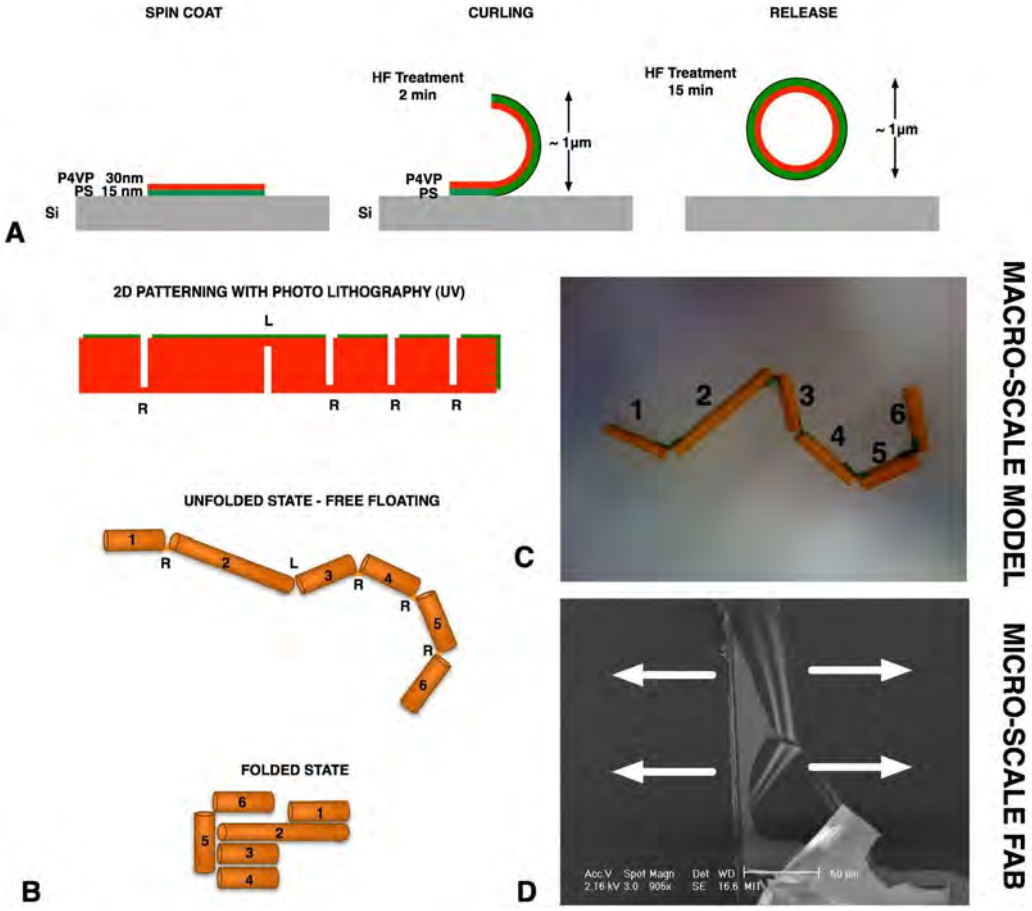

Multi-layer lithography-based folding scheme for directed folding of curled nanotubes to provide a programmable folding pattern.

Colloidal Self-Replication

The goal of this approach is to demonstrate self-replicating behavior in a new model of colloids -- "string colloids". By providing a 1D constraint for colloidal elements we can pattern or encode information along the backbone of these strings. The system is based on a tri-phase emulsion (two dispersed phases encoding ones and zeros and a continuous phase). Furthermore, the fiber backbones consist of sub-micron patterned fibers with hydrophobic and -philic patches to constrain colloidal elements to a fixed pitch. Via a screening process for a large number of candidates we have narrowed down our choice of tri-phase emulsion system and candidate sub-micron patterned fibers. Here we describe the first incubation experiments to understand the kinetics of colloid-string binding (analogous to protein-DNA binding) in this system.

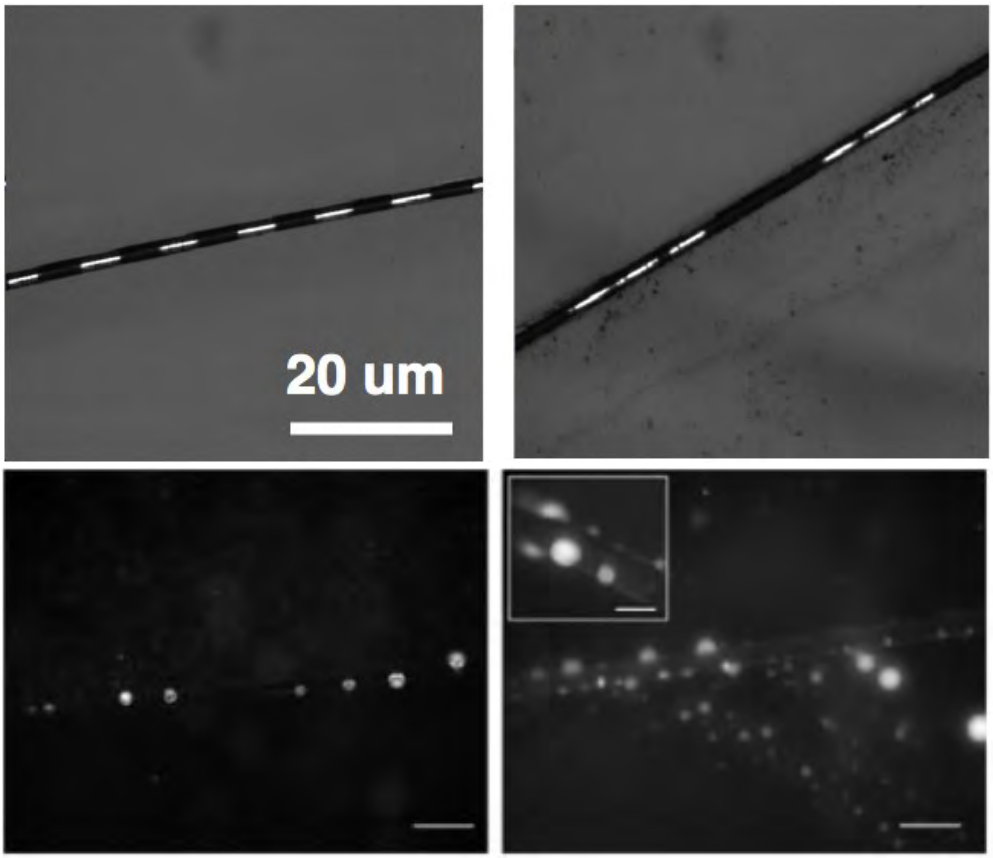

Patterned 1D bar codes embedded on glass fibers. Multi-emulsion patterning of fibers with hydrophilic and hydrophobic domains (selective and non-selective patterning).

For compatibility with biological systems the continuous phase (CP) of our tri-phase emulsion was chosen to be de-ionized water. The dispersed phase 1 (DP1) and dispersed phase 2 (DP2) form an amphiphile/oil/water system. Several class of compounds satisfy this criteria, e.g. alkanes with silicone oils in an aqueous environment. An important criteria to match in this condition is the wetting energy of DP1 and DP2, to avoid engulfment of one inside the other. This is shown in figure above

with a tri-phase emulsion with fluroescence dye in both DP1 and DP2 in an aqueous environment. The contact angle and wetting energy can be calculated from the photomicrograpgh (inset). The poly-disperse emulsion consists of droplet sizes ranging from 10 micron to sub-micron. One particular instance of this emulsion is shown in the figure (decalin/PFE/water with nile red and fluorescien dyes). For good imaging resolution, the refractive index of all components must also be matched. Furthermore, for long term stability of the emulsion, the three phases are also density matched. Experimentally we have screened several combinations of these tri-phase systems.

Droplet Fiber Networks

Extending our work on self-replicating droplet strings we have discovered a novel fluid composed of an interconnected droplet-fiber network which is an analogue of the cytoskeleton at cellular scale. These cross-linked networks spontaneously self-assemble in a mixture of patterned fibers and microscopic droplets. In this case the fibers act as an analogue to polymers like microtubule or actin and the droplets act as a binding protein (e.g. the actin binding protein ABP). Physical characteristics of this new fluid such as shear stress-strain and bulk rheology are currently being explored. We will further explore properties of this novel material introducing its reactive chemistry to implement a "programmable fluid".

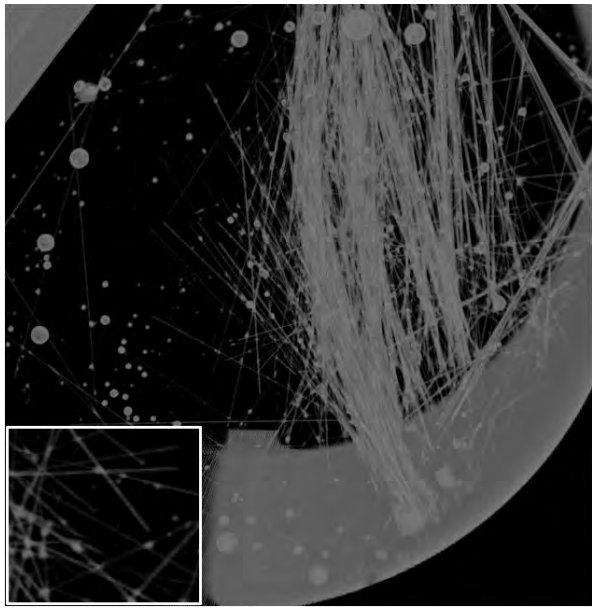

High resolution micro-CT scan of a droplet-fiber network. The architecture of the medium is characterized in three dimensions.

The fluid was prepared by introducing 5 micron diameter fibers that were several centimeter long (aspect ratio ~1000) in an oil-water emulsion with average droplet size of 10 micron. The glass fibers provide several gold binding sites for the droplets to adhere, thus forming a cross-linked tensegrity network. To visualize this network

micro-CT was employed to determine the exact location of individual fiber and emulsion droplets. It should be noted that the networks are highly organized and stable -- they were imaged continuously for ~10 hrs without any noticeable deformation.

Molecular Assembly

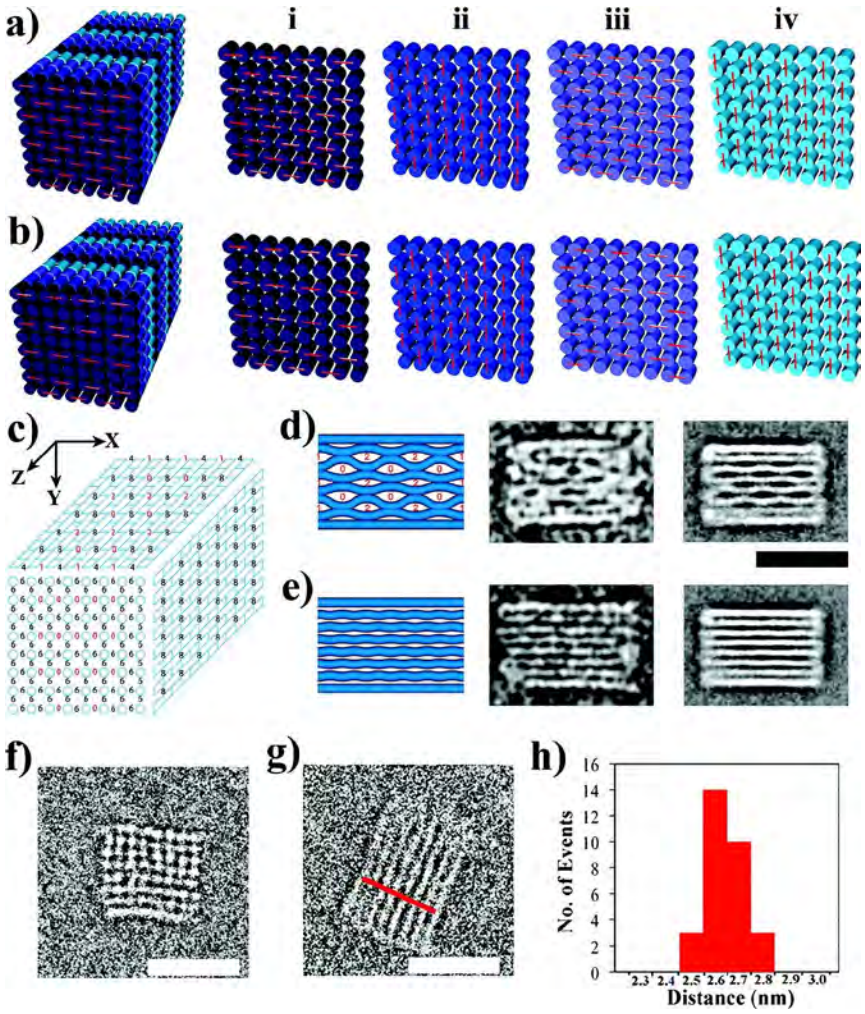

Model and transmission electron micrographs of an 8 × 8 square lattice DNA part.

We previously generalized a strategy to build custom-shaped, three-dimensional objects formed as pleated layers of helices constrained to a honeycomb lattice, with precisely controlled dimensions ranging from 10 to 100 nm. We had been working on developing a more compact design for 3D origami, with layers of helices packed on a square lattice, that can be folded successfully into structures of designed dimensions in a one-step annealing process, despite the increased density of DNA helices. A square lattice provides a more natural framework for designing rectangular structures, the option for a more densely packed architecture, and the ability to create surfaces that are more flat than is possible with the honeycomb lattice. The design and construction

of custom 3D shapes from helices packed on a square lattice thus provides a general foundational advance for increasing the versatility and scope of DNA nanotechnology.

As part of this effort, we created a new version of the CADnano DNA origami CAD software to support square lattice designs. Achieving a simple and standardized way to create designs with the new architecture has been an important step in extending the designs within our labs and also supporting the community to adopt these design patterns.

And we have developed proof-of-principle demonstrations of controlled nucleation of row-unique DNA tile lattices for in-situ molecular combing of long ssDNA scaffold strands. In this new architecture, it is not necessary to uniquely specify all of the strands in a geometrically well-defined, fully 1D-addressable DNA nanostructure. Scaffold-nucleation of unique-row ribbons is an efficient means to rigidify an ssDNA scaffold strand (auto-combing) and avoids the need to raster the scaffold strand back and forth multiple times, or to resort to an expensive all-unique tile system, in order to achieve rigidity. This enables efficient strand use and scalability for 1-dimensional self-assembly. We have demonstrated unique-row scaffolded ribbons based on single-stranded tiles, but these systems are currently limited by aggregation of the ribbons. More recently, we have demonstrated scaffolded unique-row ribbons based on double-crossover (DX) tiles, which may show a reduced tendency for aggregation.

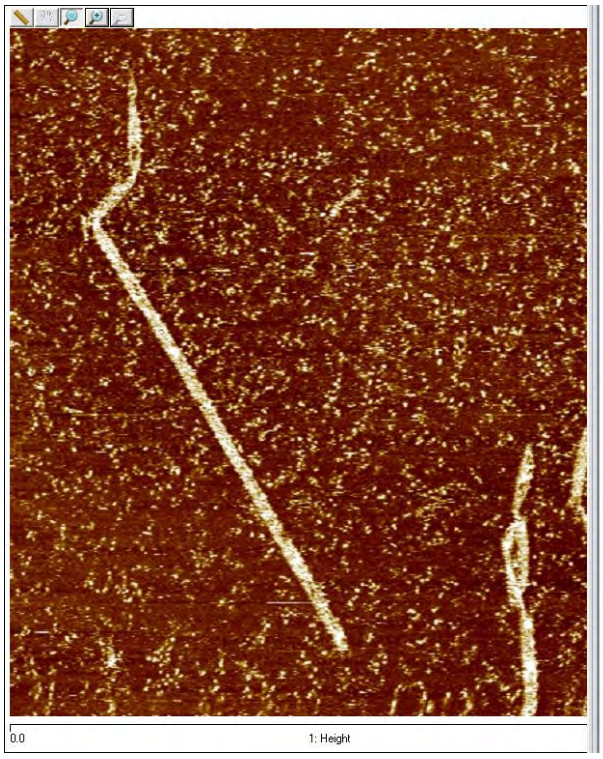

A self-assembled, non-scaffolded DNA ribbon. Integration of these systems with template strands may provide a route to fully addressable micron-scale 1D nanostructures.

Infrastructure

Project funding contributed to the establishment of required research facilities, including x-ray micro-CT scanning (X-Tek XTH160) to reconstruct programmable matter, here showing analysis of the construction of an electropermanent motor and assembly of a digital material, and precision high-speed integrated 5-axis machining (Hurco VM10U) for producing prototype motein structural components. These tools are making an important contribution to ongoing programs in these areas.

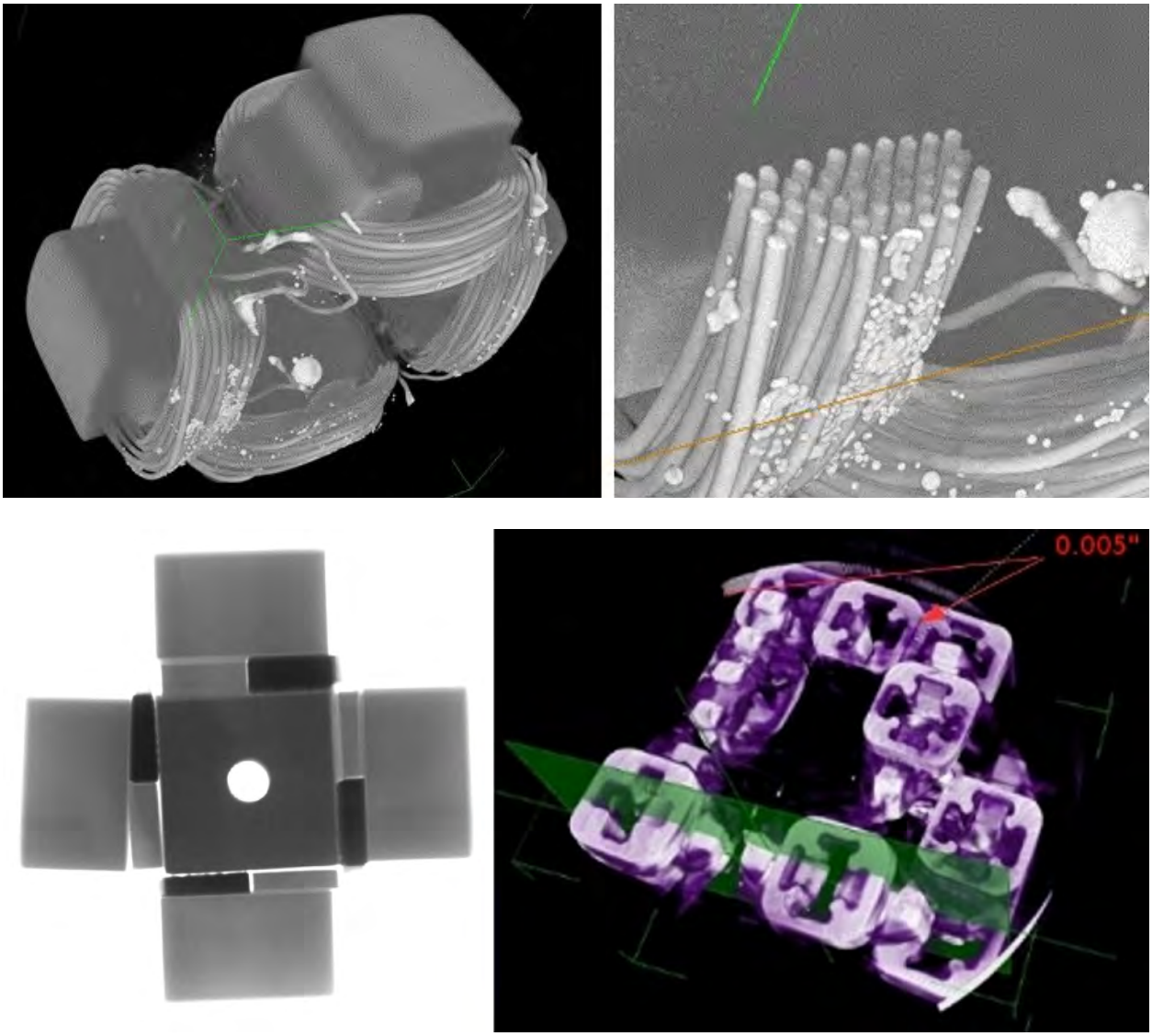

Micro-CT analysis of electropermanent stepper motor construction and digital materials for electronic interconnect.

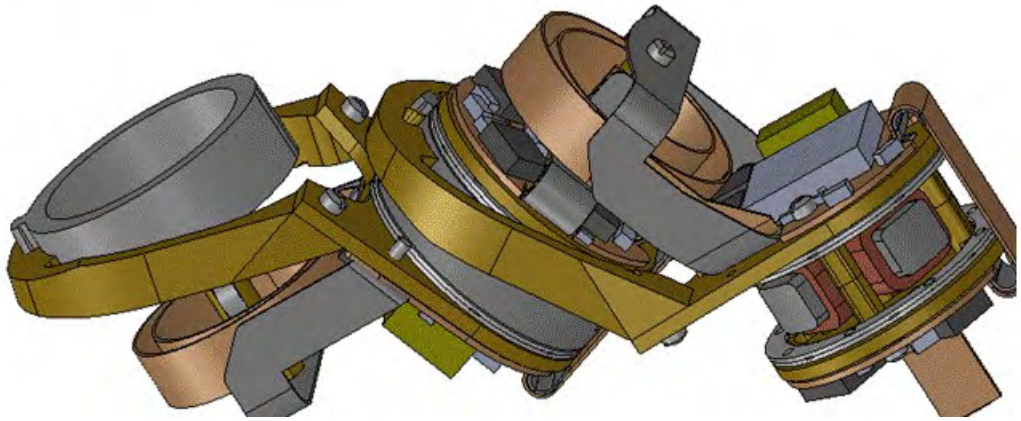

High-speed precision multi-axis machining for motein components.

Conclusions

The Programmable Matter program had the ambitious goal of creating materials that can change into arbitrary shapes. The milli-biology project has provided a research roadmap towards the realization of this vision, and in support of that developed a number of new technologies with important immediate applications.

The invention of electropermanent actuators was not anticipated in the proposal; it was a result of the challenge of integrating and scaling the motein design. There are many prospective other applications that require high torque and efficiency at low RPM in a compact volume with static holding, including flight trim and control surfaces in aerospace, and heliostat pointing for solar power. These are now transitioning to commercial development.

The milli-biology workflow for coded folding was reduced to practice in the motein family, with linked nodes providing local communication, computation, actuation, and conformation. The production of these prototypes did require significant manual assembly and was not a scalable process, but their one-dimensional mechanical and electrical construction could be automated in a continuous roll-to-roll process. This is a promising direction for future work, potentially offering low-cost reconfigurable robotics that can be supplied in arbitrary lengths.

An important direction that came from this work is externally-programmable matter, with automated assembly of functional digital materials. This satisfies the spirit rather than the letter of the programmable matter vision, providing a shorter route to the creation of materials that can be rapidly reconfigured. Development tasks include high-throughput production of the discrete components, high-speed assembly to place them, and system design with them. Once assemblers can assemble assemblers, this approach becomes analogous to the role of the ribosome in molecular biology.

Another simplification to emerge was programming surfaces rather than volumes. This focus requires the same elements of distributed computing, communications, and actuation, but enables a range of applications not originally anticipated, notably programming boundary-layer flows. This promises to have significant implications for the scalability, efficiency, and reliability of transportation. These will be investigated under the M3 program.

Publications

Programmable Assembly With Universally Foldable Strings (Moteins), K.C. Cheung, E.D. Demaine, J.R. Bachrach, and S. Griffith, IEEE Transactions on Robotics (27), pp. 718-729 (2011).

Dimensional Scaling of Switchable Electropermanent Magnets, A. Knaian, D. Rus, and N. Gershenfeld, preprint (2011).

RattleSnake: Stochastic Folding for Chain Programmable Matter, M. Lobovsky, Masters thesis, MIT (2011).

Reconfigurable Asynchronous Logic Automata: (RALA), N. Gershenfeld, D. Dalrymple, K. Chen, A. Knaian, F. Green, E. Demaine, S. Greenwald, and P. Schmidt-Nielsen, Proceedings of the 37th Annual ACM SIGPLAN-SIGACT Symposium on Principles of Programming Languages, pp. 1-6 (2010).

Electropermanent Magnetic Connectors and Actuators: Devices and Their Application in Programmable Matter, A. Knaian, Ph.D. thesis, MIT (2010).

Multi-turn, tension-stiffening catheter navigation system, Y. Chen, J.H. Chang, A.S. Greenlee, K.C. Cheung, A.H. Slocum, and R. Gupta, 2010 IEEE International Conference on Robotics and Automation (ICRA), pp. 5570-5575 (2010).

Design of Programmable Matter, A. Knaian, Masters thesis, MIT (2008).